

Impact of Timanian thrust systems on the late Neoproterozoic–Phanerozoic tectonic evolution of the Barents Sea and Svalbard

Jean-Baptiste P. Koehl^{1,2,3,4}, Craig Magee⁵, Ingrid M. Anell⁶

¹Centre for Earth Evolution and Dynamics (CEED), University of Oslo, PO Box 1028 Blindern, N-0315 Oslo, Norway.

²Department of Geosciences, UiT The Arctic University of Norway in Tromsø, N-9037 Tromsø, Norway.

³Research Centre for Arctic Petroleum Exploration (ARCEX), UiT The Arctic University of Norway in Tromsø, N-9037 Tromsø, Norway.

⁴CAGE – Centre for Arctic Gas Hydrate, Environment and Climate, UiT The Arctic University of Norway in Tromsø, N-9037 Tromsø, Norway.

⁵School of Earth Science and Environment, University of Leeds, Leeds, LS2 9JT, United Kingdom.

⁶Department of Geosciences, University of Oslo, P.O. Box 1047 Blindern, N-0316 Oslo, Norway.

Correspondence: Jean-Baptiste P. Koehl (jean-baptiste.koehl@uit.no)

Abstract

The Svalbard Archipelago consists of three basement terranes that record a complex Neoproterozoic–Phanerozoic tectonic history, including four contractional events (Grenvillian, Caledonian, Ellesmerian, and Eurekan) and two episodes of collapse- to rift-related extension (Devonian–Carboniferous and late Cenozoic). Previous studies suggest these three terranes likely accreted during the early–mid Paleozoic Caledonian and Ellesmerian orogenies. Yet recent geochronological analyses show that the northwestern and southwestern terranes of Svalbard both record an episode of amphibolite (–eclogite) facies metamorphism in the latest Neoproterozoic, which may relate to the 650–550 Ma Timanian Orogeny identified in northwestern Russia, northern Norway and the Russian Barents Sea. However, discrete Timanian structures have yet to be identified in Svalbard and the Norwegian Barents Sea. Through analysis of seismic reflection, and regional gravimetric and magnetic data, this study demonstrates the presence of continuous, several kilometers thick, NNE-dipping, deeply buried thrust systems that extend thousands of kilometers from northwestern Russia to northeastern Norway, the northern Norwegian Barents Sea, and the Svalbard Archipelago. The consistency in orientation and geometry, and apparent linkage between

these thrust systems and those recognized as part of the Timanian Orogeny in northwestern Russia and Novaya Zemlya suggests that the mapped structures are likely Timanian. If correct, these findings would imply that Svalbard's three basement terranes and the Barents Sea were accreted onto northern Norway during the Timanian Orogeny and should, hence, be attached to Baltica and northwestern Russia in future Neoproterozoic–early Paleozoic plate tectonics reconstructions. In the Phanerozoic, the study suggests that the interpreted Timanian thrust systems represented major preexisting zones of weakness that were reactivated, folded, and overprinted by (i.e., controlled the formation of new) brittle faults during later tectonic events. These faults are still active at present and can be linked to folding and offset of the seafloor.

Introduction

Recognizing and linking tectonic events across different terranes is critical to plate reconstructions. In the latest Neoproterozoic (at ca. 650–550 Ma), portions of northwestern Russia (e.g., Timan Range and Novaya Zemlya) and the Russian Barents Sea were accreted to northern Baltica by top-SSW thrusting during the Timanian Orogeny (Olovyanishnikov et al., 2000; Kostyuchenko et al., 2006). Discrete Timanian structures with characteristic WNW–ESE strikes are sub-orthogonal to the N–S-trending Caledonian grain formed during the closure of the Iapetus Ocean (Gee et al., 1994; Witt-Nilsson et al., 1998; Johansson et al., 2004; 2005). Thus far, Timanian structures have only been identified in onshore–nearshore areas of northwestern Russia and northeastern Norway and offshore in the Russian Barents Sea and southeasternmost Norwegian Barents Sea (Barrère et al., 2009, 2011; Marelllo et al., 2010; Gernigon et al., 2018; Hassaan et al., 2020a, 2020b). Therefore, the nature of basement rocks in the northern and southwestern Norwegian Barents Sea remains debatable. Some studies suggest a NE–SW-trending Caledonian suture within the Barents Sea (Gudlaugsson et al., 1998; Gee and Teben'kov, 2004; Breivik et al., 2005; Gee et al., 2008; Knudsen et al., 2019), whereas others argue for a swing into a N–S trend and merging of Norway and Svalbard's Caledonides, which probably continue into northern Greenland (Ziegler, 1988; Gernigon and Brönnert, 2012; Gernigon et al., 2014). Regardless, these models solely relate basement structures in the northern and southwestern Norwegian Barents Sea to the Caledonian Orogeny, implying that Laurentia and Svalbard were not involved in the Timanian Orogeny and were separated from Baltica by the Iapetus Ocean in the latest

Neoproterozoic (Torsvik and Trench, 1991; Cawood et al., 2001; Cocks and Torsvik, 2005; Torsvik et al., 2010; Merdith et al., 2021).

Nonetheless, geochronological data yielding Timanian ages suggest that deformation and metamorphism contemporaneous of the Timanian Orogeny affected parts of the Svalbard Archipelago and Laurentia and, possibly, all Arctic regions (Estrada et al., 2018; Figure 1a): (1) eclogite facies metamorphism (620–540 Ma; Peucat et al., 1989; Dallmeyer et al., 1990b) and eclogite facies xenoliths of mafic–intermediate granulite in Quaternary volcanic rocks are found in northern Spitsbergen (648–556 Ma; Griffin et al., 2012); (2) amphibolite facies metamorphism (643 ± 9 Ma; Majka et al., 2008, 2012, 2014; Mazur et al., 2009) and WNW–ESE-striking shear zones like the Vimsodden–Kosibapasset Shear Zone (VKSZ; Figure 1b–c) occur in southwestern Spitsbergen (600–537 Ma; Manecki et al., 1998; Faehnrich et al., 2020); and (3) xenoliths of the subduction-related Midtkap igneous suite in northern Greenland yield Timanian ages (628–570 Ma; Rosa et al., 2016; Estrada et al., 2018). In addition, several recent studies also show the presence of NW–SE- to E–W-trending basement grain in the Norwegian Barents Sea, which could possibly represent Timanian fabrics and structures (Figure 1b; Barrère et al., 2009, 2011; Marelllo et al., 2010; Klitzke et al., 2019). Following these developments, a few paleo-plate reconstructions now place Svalbard together with Baltica in the latest Neoproterozoic–Paleozoic (e.g., Vernikovsky et al., 2011), and imply that the Norwegian Barents Sea and Svalbard basement may contain Timanian structures overprinted during later (e.g., Caledonian) deformation events.

To test the origin of basement grain in the northern Norwegian Barents Sea and Svalbard, the present study focuses on several kilometers deep structures identified on 2D seismic reflection data and correlated using regional gravimetric and magnetic data. These newly identified structures trend WNW–ESE, i.e., parallel to the Timanian structural grain in northwestern Russia and northern Norway (Figure 1a–c). The structures are described and interpreted based on their geometry and potential kinematic indicators, and are compared to well-known examples of Caledonian and Timanian fabrics and structures elsewhere, e.g., onshore Norway (e.g., NNE-dipping Trollfjorden–Komagelva Fault Zone – TKFZ; Siedlecka and Siedlecki, 1967; Siedlecka, 1975), in Svalbard (e.g., gently north-plunging Atomfjella Antiform – AA; Witt-Nilsson et al., 1998), in northwestern Russia (NNE-dipping Central Timan Fault – CTF; Siedlecka and Roberts, 1995; Olovyanishnikov et al., 2000; Kostyuchenko et al., 2006), and in the southern Norwegian Barents Sea (Barrère et al., 2011; Gernigon et al., 2014) and the Russian Barents Sea (NNE-dipping

Baidaratsky fault zone – BaFZ; Lopatin et al., 2001; Korago et al., 2004; Figure 1b–c). The present contribution proposes a scenario involving several episodes of deformation starting in the Timanian Orogeny, and involving reactivation and overprinting of Timanian structures during the Caledonian Orogeny, Devonian–Carboniferous extension, Triassic extension, Eurekan tectonism, and present-day tectonism. Having established that Timanian structure may be present across the Barents Sea and Svalbard, we briefly discuss the potential implications for the tectonic evolution of the Barents Sea and the Svalbard Archipelago and associated basins (e.g., Ora and Olga basins; Anell et al., 2016).

Should our interpretation of discrete Timanian structures throughout the Norwegian Barents Sea and Svalbard be validated by future research, it would support accretion of these terranes to Baltica in the late Neoproterozoic and place the Caledonian suture farther west than is commonly suggested (e.g., Breivik et al., 2005; Gernigon et al., 2014), thus leading to a major revision of plate tectonics models. In addition, constraining the extent and reactivation history of such faults may shed some light on their influence on younger tectonic events, such as Caledonian, Ellesmerian and Eurekan contraction, Devonian–Carboniferous collapse–rifting, and late Cenozoic breakup and ongoing extension.

Geological setting

Timanian Orogeny

The Timanian Orogeny corresponds to a ca. 650–550 Ma episode of NNE–SSW contractional deformation that affected northwestern Russia and northeastern Norway. During this tectonic episode, crustal-scale, WNW–ESE-striking, NNE-dipping thrusts systems with south-southwestwards transport direction (top-SSW; Siedlecka and Siedlecki, 1967; Siedlecka, 1975; Figure 1b), accreted portions of the Russian Barents Sea and northwestern Russia onto northeastern Baltica, including Novaya Zemlya, Severnaya Zemlya, the Kanin Peninsula, the Timan Range, and the Kola Peninsula (Siedlecka and Roberts, 1995; Olovyanishnikov et al., 2000; Roberts and Siedlecka, 2002; Gee and Pease, 2004; Kostyuchenko et al., 2006; Lorenz et al., 2008; Marelllo et al., 2013) and the Varanger Peninsula in northeastern Norway (Siedlecka and Siedlecki, 1967; Siedlecka, 1975; Roberts and Olovyanishnikov, 2004; Herrevold et al., 2009; Drachev, 2016; Figure 1a). Major Timanian thrusts include the NNE-dipping Baidaratsky fault zone in the Russian Barents Sea and Novaya Zemlya (Figure 1a–b; Eldholm and Ewing, 1971, their figure 4 profile C–

D; Lopatin et al., 2001; Korago et al., 2004; Drachev, 2016), the NNE-dipping Central Timan Fault on the Kanin Peninsula and the Timan Range (Siedlecka and Roberts, 1995; Olovyanishnikov et al., 2000; Kostyuchenko et al., 2006), and the NNE-dipping Trollfjorden–Komagelva Fault Zone in northern Norway (Siedlecka and Siedlecki, 1967; Siedlecka, 1975; Herrevold et al., 2009).

Accretion of Svalbard basement terranes in the early Paleozoic

The Svalbard Archipelago consists of three Precambrian basement terranes (Figure 2), some of which show affinities with Greenland (northwestern and northeastern terranes), whereas others are possibly derived from Pearya (southwestern terrane; Harland and Wright, 1979; Ohta et al., 1989; Gee and Teben'kov, 2004; Labrousse et al., 2004; Piepjohn et al., 2013; Fortey and Bruton, 2013). These terranes possibly accreted during the mid-Paleozoic Caledonian (collision of Greenland with Svalbard and Norway at ca. 460–410 Ma; Horsfield, 1972; Dallmeyer et al., 1990a; Johansson et al., 2004, 2005; Faehnrich et al., 2020) and Late Devonian Ellesmerian orogenies (Piepjohn, 2000; Majka and Kosminska, 2017). In these models, accretion was facilitated via hundreds of kilometers of displacement along (arcuate) N–S-striking strike-slip faults, such as the Billefjorden Fault Zone (BFZ – Harland, 1969; Harland et al., 1992; Labrousse et al., 2008) and the Lomfjorden Fault Zone (LFZ – Piepjohn et al., 2019; Figure 2), although other studies suggest more limited strike-slip displacement (Lamar et al., 1986; Manby and Lyberis, 1992; Manby et al., 1994; Lamar and Douglass, 1995). Some previous workers assumed that these large (strike-slip?) faults extended thousands of kilometers southwards and represented the continuation of Caledonian faults in Scotland (Norton et al., 1987; Dewey and Strachan, 2003). Caledonian contraction resulted in the formation of large fold and thrust complexes, such as the N–S-trending, gently north-plunging Atomfjella Antiform in northeastern Spitsbergen (Gee et al., 1994; Witt-Nilsson et al., 1998) and the N–S-trending Rijpdalen Anticline in Nordaustlandet (Johansson et al., 2004; 2005; Dumais and Brönnér, 2020), whereas Ellesmerian tectonism may have formed narrow N–S-trending fold and thrust belts, like the Dickson Land and Germaniahelvøya fold-thrust zones (McCann, 2000; Piepjohn, 2000; Dallmann and Piepjohn, 2020).

In northern Norway, Timanian thrusts were reactivated–overprinted in subsequent tectonic events (e.g., Caledonian Orogeny and late–post-Caledonian collapse–rifting) as dominantly strike-to oblique-slip faults (Siedlecka and Siedlecki, 1971; Roberts et al., 1991; Herrevold et al., 2009; Rice, 2014). A notable example is the folding and reactivation of Timanian fabrics and structures

(e.g., NNE-dipping Trollfjorden–Komagelva Fault Zone) during the Caledonian Orogeny (Siedlecka and Siedlecki, 1971; Herrevold et al., 2009) and intrusion of Mississippian dolerite dykes along steeply dipping WNW–ESE-striking brittle faults that overprint the Trollfjorden–Komagelva Fault Zone onshore–nearshore northern Norway (Roberts et al., 1991; Lippard and Prestvik, 1997; Nasuti et al., 2015; Koehl et al., 2019).

Late Paleozoic post-Caledonian collapse and rifting

In the latest Silurian–Devonian, extensional collapse of the Caledonides led to the deposition of several kilometers thick sedimentary basins such as the Devonian Graben in northern Spitsbergen (Gee and Moody-Stuart, 1966; Friend et al., 1966; Friend and Moody-Stuart, 1972; Murascov and Mokin, 1979; Manby and Lyberis, 1992; Manby et al., 1994; Friend et al., 1997; McCann, 2000; Dallmann and Piepjohn, 2020). In places, N–S-trending basement ridges potentially exhumed as metamorphic core complexes along bowed, reactivated detachments, such as the Keisarhjelmen Detachment in northwestern Spitsbergen (Braathen et al., 2018).

In the latest Devonian–Mississippian, coal-rich sedimentary strata of the Billefjorden Group were deposited within normal fault-bounded basins throughout Spitsbergen (Cutbill and Challinor, 1965; Harland et al., 1974; Cutbill et al., 1976; Aakvik, 1981; Koehl and Muñoz-Barrera, 2018; Koehl, 2020a) and the Norwegian Barents Sea (Koehl et al., 2018a; Tonstad, 2018). As rift-related normal faulting evolved, Pennsylvanian sedimentation was localized into a few, several kilometers deep, N–S-trending basins like the Billefjorden Trough (Cutbill and Challinor, 1965; Braathen et al., 2011; Koehl et al., 2021 in review) and the E–W-trending Ora Basin (Anell et al., 2016). In the Permian, rift-related faulting stopped and platform carbonates were deposited throughout Svalbard (Cutbill and Challinor, 1965) and the Barents Sea (Larssen et al., 2005).

Overall, the several kilometers thick, late Paleozoic sedimentary succession deposited during late–post-Caledonian extension buried Proterozoic basement rocks. As a result, these rocks are sparsely exposed and, thus, difficult to study.

Mesozoic sedimentation and magmatism

In the Mesozoic, Svalbard and the Barents Sea remained tectonically quiet and were only affected by minor Triassic normal faulting (e.g., Anell et al., 2013; Osmundsen et al., 2014; Ogata et al., 2018; Smyrak-Sikora et al., 2020). In the Early Cretaceous, Svalbard was affected by a

regional episode of magmatism recorded by the intrusion of numerous dykes and sills of the Diabasodden Suite (Senger et al., 2013).

Early Cenozoic Eureka tectonism

The opening of the Labrador Sea and Baffin Bay between Greenland and Arctic Canada in the early Cenozoic (Chalmers and Pulvercraft, 2001; Oakey and Chalmers, 2012) led to the collision of northern Greenland with Svalbard and the formation of a fold-and-thrust belt with top-east thrusts and east-verging folds in western Spitsbergen (Dallmann et al., 1993). In eastern Spitsbergen, this deformation event is characterized by dominantly thin-skinned deformation structures, including décollements, some of which showing westwards transport directions (Andresen et al., 1992; Haremo and Andresen, 1992). Notably, the N–S-striking Agardhbukta Fault, a major splay/segment of the N–S-striking Lomfjorden Fault Zone, accommodated reverse and, possibly, strike-slip movements during this event (Piepjohn et al., 2019).

Late Cenozoic opening of the Fram Strait

After the end of extension in the Labrador Sea and Baffin Bay, the Fram Strait started to open in the earliest Oligocene (Engen et al., 2008). Tectonic extension and break-up in the Fram Strait resulted in the formation of two major, NW–SE-striking transform faults (Lowell, 1972; Thiede et al., 1990; Figure 1b).

Methods and datasets

Seismic surveys from the DISKOS database (see Figure 1b–c and supplement S1 for location) were used to interpret basement-seated structures and related, younger, brittle overprints (Figure 3a–f and Figure 4a–h and supplement S2). Other features of interest include potential dykes, which commonly appear as high positive reflections on seismic data. The geology interpreted from onshore seismic data was directly correlated to geological maps of the Norwegian Polar Institute (e.g., Dallmann, 2015). Where possible, interpretation of offshore seismic data was tied to onshore geological maps and to exploration wells Raddedalen-1 and Plurdalen-1 on Edgeøya (Bro and Shvarts, 1983; Harland and Kelly, 1997) and to the Hopen-2 well on Hopen (Anell et al., 2014; Figure 1c and supplement S3). The Raddedalen-1 well penetrated 2823 meters of Upper Permian to Mississippian or Ordovician strata, the Plurdalen well 2351 meters of Middle

Triassic to (pre-?) Devonian strata, and the Hopen-2 well 2840 meters of Middle–Upper Triassic to Pennsylvanian strata (Bro and Shvarts, 1983; Harland and Kelly, 1997; Anell et al., 2014; Senger et al., 2019). Note that the present contribution favors interpretation of lower Paleozoic (Ordovician–Silurian) rocks in the Raddedalen-1 well by Bro and Shvarts (1983) to that of upper Paleozoic (Upper Devonian–Mississippian) by Cambridge Svalbard Exploration (see contrasting interpretations in Harland and Kelly, 1997). This is based on the more detailed lithological, palynological and paleontological analyses by the former, and on the strong contrast of the lithologies described in the well with Devonian–Mississippian successions on Svalbard (Cutbill and Challinor, 1965; Cutbill et al., 1976; Friend et al., 1997; Dallmann and Piepjohn, 2020).

The present contribution only includes a few examples of seismic sections. However, more interpreted and uninterpreted seismic data are available as supplements (supplements S1–2) and from the Norwegian Petroleum Directorate (DISKOS database). None of the seismic sections were depth-converted, and thicknesses therefore appear in seconds (Two-Way Time; TWT). However, local time conversion was performed to tie seismic wells onshore Edgeøya to seismic section in Storfjorden and depth conversion was performed locally to evaluate fault displacement. Velocities of Gernigon et al. (2018) were used in these conversions. Supplement S3 includes further details related to these conversions.

The correlation of kilometer-thick structures discussed in the present contribution was also tested using gravimetric and magnetic data in cross section (Figure 3a–f) and regional magnetic and gravimetric data in the northern Norwegian Barents Sea and Svalbard (Figure 5 and supplement S4) from the Federal Institute for Geosciences and Natural Resources in Germany in map view (Klitzke et al., 2019). Regional gravimetric and magnetic data are also used to interpret deep basement fabrics and structures, e.g., regional folds (gravimetric highs commonly associated with major anticlines of thickened dense basement (i.e., Precambrian) rocks and gravimetric lows with synclines with less dense sedimentary basins) and large faults that commonly correlate with elongated gravimetric and/or magnetic anomalies (e.g., Koehl et al., 2019), and to discuss the relationship of the described structures with known structural trends in onshore basement rocks in Russia, Norway and Svalbard.

Results and interpretations

First, the interpretation of seismic data are described by area, including (1) Storfjorden (between Edgeøya and Spitsbergen) and the northeastern part of the Norwegian Barents Sea (east of Edgeøya), (2) Nordmannsfonna to Sassenfjorden onshore–nearshore the eastern–central part of Spitsbergen, and (3) the northwestern part of the Norwegian Barents Sea between Bjørnøya and Spitsbergen (Figure 1b–c). Description in each area starts with deep Precambrian basement rocks and shallow sedimentary rock units, and ends with deep brittle–ductile structures and with shallow brittle faults. Then, potential field data and regional gravimetric and magnetic anomalies in the Barents Sea and Svalbard are described, and compared and correlated to seismic data and to major Timanian and Caledonian fabrics and structures onshore northwestern Russia, Svalbard and Norway. Please see high resolution versions of all the figures and supplements on DataverseNO (doi.org/10.18710/CE8RQH).

Structures in the northwestern–northeastern Norwegian Barents Sea, Storfjorden and central–eastern Spitsbergen

Storfjorden and northeastern Norwegian Barents Sea

Folded Precambrian–lower Paleozoic basement rocks

Seismic facies at depths of 2–6 seconds (TWT) typically comprise successions of laterally discontinuous (< three kilometers long), sub-horizontal, moderately curving–undulating, moderate–high-amplitude seismic reflections that alternate with packages of highly-disrupted and/or curved low-amplitude seismic reflections (see yellow lines within pink and purple units in Figure 3a and Figure 4a). The curving geometries of the moderate–high amplitude reflections display a typical kilometer- to hundreds of meter-scale wavelength and are commonly asymmetric, seemingly leaning/verging towards the south/SSW (see yellow lines in Figure 4b). Based on ties with well bores on Edgeøya (Raddedalen-1 well; Bro and Shvarts, 1983; Harland and Kelly, 1997), these asymmetric, undulate features most likely correspond to SSW-verging folds in Precambrian–lower Paleozoic basement rocks. In places, apparent reverse offsets of these undulate reflections align along moderately–gently north- to NNE-dipping surfaces (see red lines in Figure 4a and c), which are therefore interpreted as minor, top-south/SSW, brittle thrusts.

Upper Paleozoic–Mesozoic sedimentary successions

In Storfjorden and the northwestern Norwegian Barents Sea, shallow (0–3 seconds TWT) seismic reflections above folded and thrust Precambrian–lower Paleozoic basement rocks show

significantly more continuous patterns (>> five kilometers), gently curving–undulating geometries and only local disruptions by shallow, dominantly NNE-dipping, high-angle listric disruptions (see yellow lines within orange unit in Figure 3a and c). In the northeastern Barents Sea, these reflections are largely flat-lying (see yellow lines within orange unit in Figure 3b and d). Based on field mapping campaigns and well-bores in adjacent onshore areas of Spitsbergen, Edgeøya, Hopen and Bjørnøya (see location in Figure 1b), these continuous reflections are interpreted as mildly folded upper Paleozoic–Mesozoic (–Cenozoic?) sedimentary strata (Dallmann and Krasil'scikov, 1996; Harland and Kelly, 1997; Worsley et al., 2001; Dallmann, 2015). The Permian–Triassic boundary was correlated throughout the northern Norwegian Barents Sea and Storfjorden by using the tie of Anell et al. (2014) to the Hopen-2 well.

Deep thrust systems

The packages of sub-horizontal, moderately curving–undulating (folded Precambrian–lower Paleozoic basement) reflections alternate laterally from north to south with 20–60 kilometers wide, up to four seconds thick (TWT), upwards-thickening, wedge-shaped packages (areas with high concentrations of black lines in Figure 3a and d). These wide upwards-thickening packages consist of two types of reflections. First, they include planar, continuous, gently–moderately north- to NNE-dipping, sub-parallel, high-amplitude reflections that commonly merge together downwards and that can be traced and correlated on several seismic sections in Storfjorden (black lines in Figure 3a). Upwards, these reflections terminate against high-amplitude convex-upwards reflections interpreted as intra- Precambrian–lower Paleozoic basement reflections (fuchsia lines in Figure 3a and c) or continue as moderately NNE-dipping disruption surfaces that offset these intra-basement reflections top-SSW (e.g., offset intra-Precambrian unconformities in Figure 3a and c and Figure 4d).

Second, sub-parallel, high-amplitude reflections bound wedge-shaped, upwards-thickening packages of asymmetric, curved, south- to SSW-leaning, moderately north- to NNE-dipping, moderate-amplitude reflections showing narrow (< one kilometer wide) upwards-convex geometries (Figure 4d). These asymmetric reflections also commonly appear as gently north- to NNE-dipping packages of Z-shaped reflections bounded by sub-parallel, planar, high-amplitude reflections (see yellow lines in Figure 4e). Asymmetric, south- to SSW-leaning, convex-upwards reflections are interpreted as south- to SSW-verging fold anticlines reflecting relatively low amounts of plastic deformation of layered rocks.

The alternation of packages of layered rocks folded into SSW-verging folds (yellow lines in Figure 3a–c) with packages of planar, NNE-dipping, sub-parallel, high-amplitude reflections (black lines in Figure 3a–c) suggest that the latter reflection packages represent zones where initial layering was destroyed and/or possibly reoriented, i.e., areas that accommodated larger amounts of deformation and tectonic displacement. Thus, planar, gently–moderately north- to NNE-dipping, high-amplitude reflections (black lines in Figure 3a–c) are interpreted as low-angle brittle–ductile thrust systems. We name these thrust systems (from north to south) the Steiløya–Krylen (SKFZ), Kongsfjorden–Cowanodden (KCFZ), Bellsundbanken (BeFZ), and Kinnhøgda–Daudbjørnpynten fault zones (KDFZ; Figure 3a and supplement S2a–b; see Figure 1c for location of the thrusts).

The relatively high-amplitude character of planar, NNE-dipping reflections within the thrusts suggest that these tectonic structures consist of sub-parallel layers of rocks and minerals with significantly different physical properties. A probable explanation for such laterally continuous and consistently high-amplitude reflections is partial recrystallization of rocks layers–mineral bands into rocks and minerals with significantly higher density along intra-thrust planes that accommodated large amounts of displacement (e.g., mylonitization; Fountain et al., 1984; Hurich et al., 1985). In places, packages of aggregates of Z-shaped reflections bounded upwards and downwards by individual low-angle thrust surfaces are interpreted as forward-dipping duplex structures (e.g., Boyer and Elliott, 1982) reflecting relatively strong plastic deformation between low-angle, brittle–ductile (mylonitic?) thrusts (see yellow lines in Figure 4e).

The Kongsfjorden–Cowanodden, Bellsundbanken, and Kinnhøgda–Daudbjørnpynten fault zones can be traced east-southeast of Edgeøya as a similar series of 20–60 kilometers wide, up to four seconds thick (TWT), upwards-thickening packages (e.g., black lines in Figure 3d and supplements S2a). However, their imaging along NNW–SSE-trending seismic sections is much more chaotic and it is more difficult to identify smaller structures (like south-verging folds and minor thrusts) within each thrust system (e.g., supplement S2a). This suggests that these three thrust systems strike oblique to NNW–SSE-trending seismic sections (supplement S2a), whereas they are most likely sub-orthogonal to N–S- to NNE–SSW-trending seismic sections in Storfjorden (Figure 3a). The only orientation that reconciles these seismic facies variations (i.e., well-imaged on NNE–SSW-trending seismic sections and poorly imaged by NNW–SSE-trending seismic sections; Figure 3a and supplement S2a) is an overall WNW–ESE strike.

South of each 20–60 kilometers wide packages of thrust surfaces and related fold and duplex structures, seismic reflections representing Precambrian–lower Paleozoic basement rocks typically appear as gently curved, convex-upwards, relatively continuous reflections showing sub-horizontal seismic onlaps (see white arrows in Figure 3a–f). This suggests that Precambrian–lower Paleozoic basement rocks most likely consist (meta-) sedimentary rocks (analogous to those observed in northeastern Spitsbergen and Nordaustlandet; Harland et al., 1993; Stouge et al., 2011) that were deposited in foreland and piggy-back basins ahead of each 20–60 kilometers wide packages (Figure 3a–f).

Hence, based on the upwards-thickening geometry of the packages of south- to SSW-verging folds and of forward-dipping duplexes, on the top-SSW reverse offsets of intra-basement reflections by low-angle brittle–ductile thrust surfaces, on the upwards truncation of these low-angle thrusts by intra-basement reflections, and on the onlapping geometries of (meta-) sedimentary basement rocks south of each set of top-SSW thrust surfaces, the 20–60 kilometers wide, upwards-thickening, wedge-shaped packages are interpreted as crustal-scale, several kilometers thick, north- to NNE-dipping, top-SSW, brittle–ductile thrust systems (see fault zones with high concentration of black lines in Figure 3a–f). These thrust systems include low-angle, brittle–ductile, mylonitic thrust surfaces (black lines in Figure 4d–e) separating upwards-thickening thrust sheets that consist of gently to strongly folded basement rocks and forward-dipping duplex structures (yellow lines in Figure 4d–e). These thrust sheets are interpreted to reflect accretion and stacking from the north or north-northeast. The interpreted thrust systems are comparable in seismic facies and thickness to kilometer-thick mylonitic shear zones in the Norwegian North Sea (Phillips et al. 2016) and southwestern Norwegian Barents Sea (Koehl et al., 2018).

N–S-trending folds

On E–W seismic cross sections, reflections of the Kongsfjorden–Cowanodden, Bellsundbanken, and Kinnhøgda–Daudbjørnpynnten fault zones define large, 50–100 kilometers wide, U-shaped, symmetrical depressions (black lines in Figure 3b) on the edge of which they are truncated at a high angle and overlain by folded lower Paleozoic and mildly folded to flat-lying upper Paleozoic (meta-) sedimentary rocks (purple and orange units with associated yellow lines in Figure 3b). In addition, within these U-shaped depressions, the thrust systems show curving up and down, symmetrical geometries with 5–15 kilometers wavelength (yellow lines within the pink

unit in Figure 3b and Figure 4f). Also notice the kilometer- to hundreds of meter-scale undulating pattern of 5–15 kilometers wide curved geometries (yellow lines in Figure 4f). Based on the truncation and abrupt upward disappearance of high-amplitude seismic reflections characterizing the thrust systems, the high-angle truncation of the thrusts is interpreted as a major erosional unconformity (dark blue line in Figure 3b and pink line in Figure 4f), and the large U-shaped depressions as large N–S- to NNE–SSW-trending, upright regional folds (black lines in Figure 3b). Furthermore, the 5–15 kilometers wide, symmetrical, curved geometries and associated, kilometer- to hundreds of meter-scale, undulating pattern of seismic reflections within the thrusts are interpreted as similarly (N–S- to NNE–SSW-) trending, upright, parasitic macro- to meso-scale folds (yellow lines in Figure 3b and Figure 4f).

Shallow brittle faults

In places, near the top of the 20–60 kilometers wide thrust systems (Kongsfjorden–Cowanodden, Bellsundbanken, and Kinnhøgda–Daudbjørnpynten fault zones), low-angle brittle–ductile thrust surfaces merge upwards with high-angle to vertical, listric, north- to NNE-dipping disruption surfaces at depths of c. 2–3 seconds (TWT; see red lines in Figure 3a and d). These listric disruption surfaces truncate shallow, laterally continuous reflections that display gently curved, symmetric geometries in Storfjorden (yellow lines in Figure 3a) and flat-lying geometries in the northeastern Norwegian Barents Sea (yellow lines in Figure 3d). Notably, they show minor, down-NNE normal offsets, and related minor southwards thickening (towards the disruption) of seismic sub-units within Devonian–Carboniferous (–Permian?) sedimentary strata in the north, both in Storfjorden and the northeastern Barents Sea (Figure 3a–d and white double arrows in Figure 4g). In addition, they display minor reverse offsets and associated gentle upright folding of shallow continuous reflections potentially representing upper Mesozoic (–Cenozoic?) sedimentary deposits in Storfjorden (Figure 3a–c and e, and orange lines in Figure 4h). Note that flat-lying Mesozoic (–Cenozoic?) sedimentary rocks are not offset in the northeastern Norwegian Barents Sea (Figure 3d).

Based on the observed normal offsets and southwards-thickening of Devonian–Carboniferous (–Permian?) sedimentary strata north of these disruption surfaces (e.g., white double arrows in Figure 4g), these are interpreted as syn-sedimentary Devonian–Carboniferous normal faults. The minor reverse offsets and associated gentle upright folding of Mesozoic (–Cenozoic?) sedimentary rocks in Storfjorden (e.g., orange lines in Figure 4h) suggest that these normal faults

were mildly inverted near Svalbard in the Cenozoic. However, it is unclear whether inversion in Storfjorden initiated in the early Cenozoic or later. Nonetheless, minor reverse offset and folding of the seafloor clearly indicate ongoing inversion along these faults (Figure 3a and c, and Figure 4h). Furthermore, considering the merging relationship between these high-angle listric disruption surfaces and underlying shear zones (i.e., merging black and red lines in Figure 3a and c–d), we propose that the formation of Devonian–Carboniferous normal faults was controlled by the crustal-scale, north- to NNE-dipping (inherited) thrust systems (Kongsfjorden–Cowanodden, Bellsundbanken, and Kinnhøgda–Daudbjørnpynten fault zones).

Nordmannsfonna–Sassenfjorden (eastern–central Spitsbergen)

Deep thrust system and N–S-trending folds

Seismic data from Nordmannsfonna to Sassenfjorden in eastern Spitsbergen (see Figure 1c for location) show reflection packages including both planar, continuous, moderately-dipping high-amplitude reflections and upwards-curving, moderate-amplitude reflections (black and yellow lines in Figure 3e–f). These two sets are similar to reflection packages interpreted as low-angle, brittle–ductile mylonitic thrusts bounding packages of south- to SSW-verging folds in Storfjorden and the northeastern Norwegian Barents Sea (black and yellow lines in Figure 3a and d, and supplement S2a). In addition, they are located at similar depths (> 2 seconds TWT) and seem to align with the Kongsfjorden–Cowanodden fault zone in Storfjorden along a WNW–ESE-trending axis. Hence, we interpret the deep, continuous, high-amplitude reflections in eastern Spitsbergen as the western continuation of the top-SSW Kongsfjorden–Cowanodden fault zone. This thrust can be traced on seismic data as gently NNE-dipping, high-amplitude reflections in Sassendalen and Sassenfjorden–Tempelfjorden (supplement S2c–d), and possibly in Billefjorden (Koehl et al., 2021 in review, their figure 9a–b).

In Nordmannsfonna, the base-Pennsylvanian unconformity (white line in Figure 3e–f; tied to onshore geological maps; Dallmann, 2015) truncates the Kongsfjorden–Cowanodden fault zone (black lines in Figure 3e–f) upwards and the fault shows pronounced variations in dip direction, ranging from east-dipping in the east to NNE-dipping in the north and WNW-dipping in the west, which result into a c. 15–20 kilometers wide, north- to NNE-plunging dome-shaped/convex-upwards geometry (black lines in Figure 3e–f). This portion of the thrust system is interpreted to

be folded into a major NNE- to north-plunging upright fold, whose 3D geometry was accurately constrained due to good seismic coverage in this area (Figure 1c).

Small-scale structures within the Kongsfjorden–Cowanodden fault zone also show asymmetric folds and internal seismic units terminating upwards with convex-upwards reflections (yellow lines in Figure 3e–f) suggesting top-SSW nappe thrusting in the northern portion of the thrust system. However, on E–W cross sections, seismic data reveal a set of west-verging folds in the east and a more chaotic pattern of symmetrical, dominantly upright folds in the west (yellow lines in Figure 3e) and below a major, high-angle, east-dipping disruption surface (thick red line in Figure 3e) that crosscuts the Kongsfjorden–Cowanodden fault zone.

Shallow brittle faults

The high-angle, east-dipping disruption surface (thick red line in Figure 3e) is associated with minor subvertical to steeply east-dipping disruption surfaces (thin red lines in Figure 3e). This feature shows a major reverse, top-west offset (> 0.5 second TWT) of seismic units and reflections at depth > 0.75 second (TWT; e.g., black lines in Figure 3e), and minor reverse offset (< 0.1 second TWT) and upwards-convex curving of adjacent reflections at depth < 0.75 second (TWT; white line and yellow lines within blue and units in Figure 3e). Since the major disruption coincides with the location of the Agardhbukta Fault (Piepjohn et al., 2019; see Figure 1 for location) and shows a steep inclination near the surface similar to that of the Agardhbukta Fault, it is interpreted as the subsurface expression of this fault. The Agardhbukta Fault offsets the Kongsfjorden–Cowanodden fault zone in a reverse fashion (> 0.5 second TWT; black lines in Figure 3e), and terminates upwards within and slightly offsets upper Paleozoic–Mesozoic sedimentary rocks (blue and black units and associated yellow lines in Figure 3e), which were correlated to onshore outcrops in eastern Spitsbergen (Andresen et al., 1992; Haremo and Andresen, 1992; Dallmann, 2015). As a result, these rocks are folded into a N–S-trending, open, upright fold around the fault tip, both of which suggest top-west movements along the fault (Figure 3e).

Pre-Pennsylvanian dykes

In the hanging wall and on the eastern flank of the folded Kongsfjorden–Cowanodden fault zone in Nordmannsfonna, high- to low-amplitude, gently east-dipping seismic reflections, which possibly represent sedimentary strata (light orange unit in Figure 3e), are crosscut but not offset by moderately west-dipping, high-amplitude planar reflections (blue lines in Figure 3e). In NNE–SSW-trending cross-sections, these high-amplitude, cross-cutting seismic reflections appear sub-

horizontal (blue lines in Figure 3f). These crosscutting, west-dipping reflections are mildly folded in places and either terminate upwards within the suggested, gently east-dipping, sedimentary strata (light orange unit in Figure 3e) or are truncated by the base-Pennsylvanian unconformity (white line in Figure 3e). Downwards within the Kongsfjorden–Cowanodden fault zone (black lines in Figure 3e), these inclined reflections can be vaguely traced as a series of discontinuous, subtle features (see blue lines in Figure 3e). In the footwall of the Kongsfjorden–Cowanodden fault zone, the inclined reflections become more prominent again, still do not offset background reflections, and extend to depths of 3–3.5 seconds (TWT; blue lines in Figure 3e). The high amplitude of these planar west-dipping reflections, the absence of offset across them, and their discontinuous geometries across the Agardhbukta Fault and the Kongsfjorden–Cowanodden fault zone suggest that they may represent dykes (see Phillips et al., 2018). Because they appear truncated by the Base-Pennsylvanian unconformity, we suggest such dykes were emplaced prior to development of this unconformity. The Kongsfjorden–Cowanodden fault zone is folded into a broad, 15–20 kilometers wide anticline, and offset > 0.5 second (TWT) by the Agardhbukta Fault, whereas the west-dipping dykes (blue lines in Figure 3e) and the gently east-dipping sedimentary strata they intrude (light orange unit in Figure 3e) are only mildly folded and show no offset across the Agardhbukta Fault (Figure 3e). These differences in deformation suggest that the latter were deformed during a mild episode of late contraction but not by the same early episode of intense contraction that resulted in macrofolding of the Kongsfjorden–Cowanodden fault zone.

Cretaceous dykes and sills

Near or at the surface, thin, kilometer-wide, lenticular packages of gently dipping, moderate–high-amplitude seismic reflections (black units in Figure 3e–f) correlate with surface outcrops of Cretaceous sills of the Diabasodden Suite in eastern Spitsbergen (Senger et al., 2013; Dallmann, 2015). In places, these sills are associated with areas showing high-frequency disruptions of underlying sub-horizontal seismic reflections (dotted black lines in Figure 3f) correlated with onshore occurrences of Pennsylvanian–Mesozoic sedimentary strata (Andresen et al., 1992; Haremo and Andresen, 1992; Dallmann, 2015). We interpret these areas of high-frequency disruption in otherwise relatively undisturbed and only mildly deformed Pennsylvanian–Mesozoic sedimentary strata as zones with occurrences of Cretaceous feeder dykes. Alternatively, disruption may be related to scattering and attenuation of seismic energy caused on the sills.

Stappen High (northwestern Norwegian Barents Sea north of Bjørnøya)

On the Stappen High between Bjørnøya and Spitsbergen (Figure 1c), seismic reflections at depth of 2–6 seconds (TWT) are dominated by moderate- to high-amplitude reflections with limited (< five kilometers) lateral continuity showing asymmetric, dominantly SSW-leaning curving geometries with a few hundreds of meters to a few kilometers width (yellow lines within pink unit in Figure 3c), i.e., analogous to those in folded Precambrian basement rocks farther north (Figure 3a and Figure 4a). These reflections are truncated by gently to moderately NNE- (and subsidiary SSW-) dipping disruption surfaces (black lines within pink and purple units in Figure 3c), some of which connect upwards with shallow (0–2 seconds TWT), NNE-dipping, high-angle listric disruptions near Bjørnøya in the south (red lines in Figure 3c). Notably, major seismic reflections near the upwards termination of deep, moderately–gently NNE-dipping disruption surfaces display characteristic gently curving-upwards geometries (yellow lines within pink and purple units in Figure 3c) and overlying seismic onlaps (white half arrows in Figure 3c) similar to those observed just south of major NNE-dipping thrust systems in Storfjorden and the northeastern Norwegian Barents Sea (Figure 3a and supplement S2).

We interpret deep (2–6 seconds TWT), curving, discontinuous seismic reflections ((yellow lines within pink and purple units in Figure 3c) as folded Precambrian–lower Paleozoic basement rocks, and dominantly NNE-dipping disruption surfaces (black lines within pink and purple units in Figure 3) as brittle–ductile thrust possibly partly mylonitic, though with less intense deformation than the major NNE-dipping thrust systems observed farther north in Storfjorden and the northeastern Norwegian Barents Sea, like the Kongsfjorden–Cowanodden fault zone. These brittle–ductile thrusts can be traced eastwards on seismic data on the Stappen High and into the Sørkapp Basin (Figure 1c).

Based on their geometries and on gentle folding of the seafloor reflection (yellow lines within green unit in Figure 3c), shallow, NNE-dipping, high-angle listric disruptions are interpreted as mildly inverted normal faults overprinting deep NNE-dipping thrusts. Based on previous fieldwork on Bjørnøya (Worsley et al., 2001), on seismic mapping in the area (Lasabuda et al., 2018), and on well tie to Hopen and Edgeøya, relatively continuous (> five kilometers) shallow (0–2 seconds TWT), gently curved–undulating seismic reflections overlying folded Precambrian–lower Paleozoic basement rocks are interpreted as mildly folded upper Paleozoic–Mesozoic (–Cenozoic?) sedimentary strata (orange and green units in Figure 3c).

Potential field data and regional gravimetric and magnetic anomalies
NNE-dipping thrusts

In the northern Barents Sea, Storfjorden and central–eastern Spitsbergen, the seismic occurrences of the Kongsfjorden–Cowanodden, Bellsundbanken and Kinnhøgda–Daudbjørnpynten fault zones coincide with gradual, step-like, southwards increases in gravimetry and, in places, with high magnetic anomalies in cross-section (Figure 3a–b and d–f). Similar southwards gradual and step-like increases in the Bouguer and magnetic anomalies correlate with major thrusts north of Bjørnøya (Figure 3c; see Figure 1b for location of Bjørnøya). These patterns suggest that the footwall of the thrust systems consists of relatively denser rock units. Seismic interpretation showing thickening of metamorphosed and folded Precambrian basement rock units (pink unit in Figure 3a and c–d) in the footwall of the thrusts further support this claim.

In map-view gravimetric and magnetic data, the three thrust systems in Storfjorden (black lines in Figure 3a) coincide with three high, WNW–ESE-trending, continuous, gently undulating (and, in place, merging/splaying) gravimetric and discontinuous magnetic anomalies (dashed yellow lines in Figure 5a–c) that are separated from each other by areas showing relatively low gravimetric and magnetic anomalies (e.g., see green to blue areas in Figure 5a). Some of these anomalies extend from central Spitsbergen to Storfjorden and the northern Barents Sea (below the Ora and Olga basins) as curving, E–W- and NW–SE-trending, 50–100 kilometers wide anomalies (dashed yellow lines in Figure 5a–c). Analogously, thrust systems north of Bjørnøya (Figure 3c) and north of the Ora and Olga basins (supplement S2b) correlate with comparable WNW–ESE-trending, curving magnetic and gravimetric anomalies (dashed yellow lines in Figure 5a–c). The WNW–ESE-trending anomalies appear clearer by using a slope-direction shader for gravimetric data, which accentuates the contrast between each trend of anomalies (green and red areas in Figure 5b).

Most of the recognized, regional WNW–ESE-trending magnetic and gravimetric anomalies (dashed yellow lines in Figure 5a–c) can be traced into the Russian Barents Sea where they are linear and are crosscut by major N–S- to NNW–SSE-trending anomalies (dashed black and white lines in Figure 5a–c). Subtle WNW–ESE-trending magnetic and gravimetric anomalies further extend onshore northwestern Russia (e.g., Kanin Peninsula and southern Novaya Zemlya) where they correlate with major Timanian thrusts and folds, some of which are suspected to extend

thousands of kilometers between northwestern Russia and the Varanger Peninsula in northern Norway (e.g., Trollfjorden–Komagelva Fault Zone and Central Timan Fault; Siedlecka, 1975; Siedlecka and Roberts, 1995; Olovyanishnikov et al., 2000; Kostyuchenko et al., 2006). In addition, two of the southernmost WNW–ESE-trending gravimetric and magnetic anomalies coincide with the location of well known, crustal-scale, SSW-verging Timanian thrust faults, the Trollfjorden–Komagelva Fault Zone and the Central Timan Fault. Thus, based on their overall WNW–ESE trend, patterns of alternating highs and lows both for gravimetric and magnetic anomalies (see Figure 5a), location at the boundary of oppositely dipping slopes (see slope-direction shader map in Figure 5b), and extensive field studies and seismic and well data in northwestern Russia (e.g., Kanin Peninsula and Timan Range; Siedlecka and Roberts, 1995; Olovyanishnikov et al., 2000; Kostyuchenko et al., 2006) and northern Norway (e.g., Varanger Peninsula; Siedlecka, 1975), WNW–ESE-trending anomalies are interpreted as a combination of basement-seated Timanian macrofolds and top-SSW reverse faults (Figure 5a–c).

N–S-trending folds

Large N–S-trending open folds (e.g., black and yellow lines in Figure 3b) coincide with N–S- to NNE–SSW-trending, 20–100 kilometers wide, arcuate gravimetric and magnetic anomalies (dashed white and black lines in Figure 5a–c), which are highly oblique to WNW–ESE-trending gravimetric and magnetic anomalies and thrust systems (dashed yellow lines in Figure 5a–c). Notably, major N–S- to NNE–SSW-trending synclines in Figure 3b (marked as red lines over a white line in Figure 5a and c and as pink lines over a red line in Figure 5b) coincides with similarly trending gravimetric and magnetic anomalies (dashed black lines in Figure 5a and c and dashed white lines in Figure 5b). On the slope-direction shader map of gravimetric data, these N–S- to NNE–SSW-trending anomalies are localized along the boundary between areas with eastwards- (ca. 90–100°; blue areas in Figure 5b) and westwards-facing slopes (ca. 270–280°; white areas in Figure 5b).

Notably where the main thrusts are preserved, major N–S-trending synforms (see 50–60 kilometers wide U-shaped depression formed by the Kinnhøgda–Daudbjørnpynten fault zone, i.e., black lines, in Figure 3b) coincide with gravimetric and magnetic highs (white and black dashed lines in Figure 5a–c), whereas major antiforms where major NNE-dipping thrusts are partly eroded (e.g., c. 100 kilometers wide areas where the Kinnhøgda–Daudbjørnpynten fault zone is absent in

Figure 3b) coincide with gravimetric and magnetic lows (the lows are parallel to white and black dashed lines symbolizing magnetic and gravimetric highs in Figure 5a–c). The correlation of the interpreted NNE-dipping thrust systems with gravimetric highs suggests that the thrusts consist of relatively denser rocks. This supports the inferred mylonitic component of the thrusts because mylonites are relatively denser due to the formation of high-density minerals with increasing deformation (e.g., Arbaret and Burg, 2003; Colombu et al., 2015).

In the northwestern part of the Barents Sea (i.e., area covered by seismic data presented in Figure 3), N–S- to NNE–SSW-trending gravimetric and magnetic anomalies (white and black dashed lines in Figure 5a–c) are typically 20–50 kilometers wide and correlate with similarly trending Caledonian folds and thrusts onshore Nordaustlandet (e.g., Rijpdalen Anticline; Johansson et al., 2004; 2005; Dumais and Brönnner, 2020) and northeastern Spitsbergen (e.g., Atomfjella Antiform; Gee et al., 1994; Witt-Nilsson et al., 1998), whose width is comparable to that of the anomalies. In the south, N–S- to NNE–SSW-trending gravimetric and magnetic anomalies merge together and swing into a NE–SW trend onshore–nearshore the Kola Peninsula and northern Norway. These anomalies mimic the attitude of Caledonian thrusts and folds in the southern Norwegian Barents Sea (Gernigon and Brönnner, 2012; Gernigon et al., 2014) and onshore northern Norway (Sturt et al., 1978; Townsend, 1987; Roberts and Williams, 2013). In the east, N–S- to NNE–SSW-trending anomalies broaden to up to 150 kilometers in the Russian Barents Sea (Figure 5a–c).

In places, the intersections of high, WNW–ESE- and N–S- to NNE–SSW-trending gravimetric and magnetic anomalies generate relatively higher, oval-shaped anomalies (e.g., dotted white lines in Figure 5a and c). Notable examples are found in the Ora and Olga basins and east and south of these basins (see dotted white lines in Figure 5a and c).

Discussion

In the discussion, we consider the lateral extent of the interpreted NNE-dipping thrust systems, their possible timing of formation, and potential episodes of reactivation and overprinting. Then we briefly discuss the implications of these thrust systems for plate tectonics reconstructions in the Arctic.

Extent of NNE-dipping thrust systems

Four major NNE-dipping systems of mylonitic thrusts and shear zones (Steiløya–Krylen, Kongsfjorden–Cowanodden, Bellsundbanken, Kinnhøgda–Daudbjørnpynten fault zones) were identified at depths > 1–2 seconds (TWT) in central–eastern Spitsbergen, Storfjorden and the northeastern Barents Sea, and several systems with less developed ductile fabrics between Spitsbergen and Bjørnøya on the Stappen High (Figure 3a–f).

The Kongsfjorden–Cowanodden fault zone is relatively easy to trace and correlate in Sassenfjorden, Sassendalen, Nordmannsfonna, Storfjorden and the northeastern Barents Sea (east of Edgeøya) because (i) the seismic data in these areas have a high resolution and good coverage, (ii) internal seismic reflections are characterized by high amplitudes (e.g., brittle–ductile thrusts and mylonitic shear zones), (iii) kinematic indicators within the thrust system consistently show dominantly top-SSW sense of shear with SSW-verging fold structures (Figure 3a and d–f, and supplement S2), (iv) the geometry and kinematics indicators along shallow brittle overprints are regionally consistent (listric, down-NNE, brittle normal faults; Figure 3a and d–f), and (v) this thrust consistently coincides with increase in gravimetric and magnetic anomaly in cross-section (Figure 3a and d) and with analogously trending gravimetric and magnetic anomalies in central–eastern Spitsbergen and the northern Barents Sea (Figure 5a–b). This thrust system was previously identified below the Ora Basin by Klitzke et al. (2019), though interpreted as potential Timanian grain instead of a discrete structure. The proposed correlation based on seismic, and cross-section and map-view gravimetric and magnetic data suggests a lateral extent of c. 550–600 kilometers along strike for the Kongsfjorden–Cowanodden fault zone. However, the regional magnetic and gravimetric anomalies associated with this thrust in the Norwegian Barents Sea and Svalbard extend potentially farther east as a series of WNW–ESE-trending anomalies to the mainland of Russia (Figure 5a–c). Notably, these anomalies correlate with the southern edge of Novaya Zemlya (Figure 5a–c) and, more specifically, with WNW–ESE-striking fault segments of the Baidaratsky fault zone (Figure 1a; Lopatin et al., 2001; Korago et al., 2004), a major thrust fault that bounds a major basement high in the central Russian Barents Sea, the Ludlov Saddle (Johansen et al., 1992; Drachev et al., 2010). Thus, it is possible that the Kongsfjorden–Cowanodden fault zone also extends farther east, possibly merging with the Baidaratsky fault zone, i.e., with a minimum extent of 1700–1800 kilometers (Figure 5a–c).

The overall NNE-dipping and folded (into NNE-plunging folds) geometry of the Kongsfjorden–Cowanodden fault zone (Figure 3e–f and Klitzke et al., 2019, their figures 3–5) may

explain the alternating NW–SE- and E–W-trending geometry of the gravimetric and magnetic anomalies correlating with this thrust system (Figure 5a–b). E–W- and NW–SE-trending segments of these anomalies may represent respectively the western and eastern limbs of open, gently NNE-plunging macro-anticlines in the northern Norwegian Barents Sea. The relatively higher, oval-shaped gravimetric and magnetic anomalies at the intersection of WNW–ESE- and N–S- to NNE–SSW-trending magnetic and gravimetric highs, which are interpreted as the interaction of two sub-orthogonal fold trends further support this claim (Figure 5a and c).

Interpretation of seismic sections (Figure 3e–f and supplement S2) and regional magnetic and gravimetric data (Figure 5a–c) in central–eastern Spitsbergen show that NNE-dipping, top-SSW Kongsfjorden–Cowanodden and Bellsundbanken fault zones likely extend westwards into central (and possibly northwestern) Spitsbergen (e.g., Sassendalen, Sassenfjorden, Tempelfjorden, and Billefjorden; see Figure 1c for locations). This is further supported by recent field, bathymetric and seismic mapping in central Spitsbergen showing that (inverted) Devonian–Carboniferous NNE-dipping brittle normal faults in Billefjorden and Sassenfjorden–Tempelfjorden merge with kilometer-scale, NNE-dipping, Precambrian basement fabrics and shear zones at depth (Koehl, 2020a; Koehl et al., 2021 in review). Other examples of WNW–ESE-trending fabrics include faults within Precambrian basement and Carboniferous sedimentary rocks in northeastern Spitsbergen (Witt-Nilsson et al., 1998; Koehl and Muñoz-Barrera, 2018), and within Devonian sedimentary rocks in northern and northwestern Spitsbergen (Friend et al., 1997; McCann, 2000; Dallmann and Piepjohn, 2020). These suggest a repeated and regional influence of WNW–ESE-trending thrust systems and associated basement fabrics in Spitsbergen.

Analogously to the Kongsfjorden–Cowanodden fault zone, the Bellsundbanken and Kinnhøgda–Daudbjørnpynten fault zones (Figure 3a) geometries and kinematics on seismic data, and their coinciding with parallel gravimetric and magnetic anomalies in map view and with magnetic and gravimetric highs in cross-section suggest that they extend from Storfjorden to the island of Hopen (Figure 1c, Figure 3a, Figure 5a–c, and supplement S2). Notably, a 50–100 kilometers wide, NNE–SSW-trending gravimetric and associated magnetic anomaly interpreted as Caledonian grain in Nordaustlandet (Rijpdalen Anticline; Dumais and Brönnner, 2020) bends across the trace of these two thrust systems (Figure 5a–c). Farther east, the Bellsundbanken and Kinnhøgda–Daudbjørnpynten fault zones parallel gravimetric and magnetic, alternating E–W- and NW–SE-trending anomalies that follow the trends and map-view shapes of the Ora and Olga basins

in the northeastern Norwegian Barents Sea (Anell et al., 2016; see Figure 1b–c for location). This suggests that these two thrust systems extend into the northeastern Norwegian Barents Sea and, potentially, into the Russian Barents Sea, and affected the development of Paleozoic sedimentary basins. This is also the case of the Steiløya–Krylen fault zone (supplement S2b), which coincides with mild, discontinuous, WNW–ESE-trending gravimetric and magnetic anomalies that extend well into the Russian Barents Sea and, possibly, across Novaya Zemlya (Figure 5a–c).

In southwestern Spitsbergen, field mapping revealed the presence of a major, subvertical, kilometer-thick, WNW–ESE-striking mylonitic shear zone metamorphosed under amphibolite facies conditions, the Vimsodden–Kosibapasset Shear Zone (Majka et al., 2008, 2012; Mazur et al., 2009; see Figure 1c for location). This major sinistral shear zone aligns along a WNW–ESE-trending axis with the Kinnhøgda–Daudbjørnpynten fault zone in the northwestern Norwegian Barents Sea (Figure 3a), and shows a folded geometry in map view that is comparable to that of major NNE-dipping thrust systems in the northern Norwegian Barents Sea (Figure 3a and e–f, Figure 5a–c, and supplement S2; Klitzke et al., 2019). In addition, the Vimsodden–Kosibapasset Shear Zone juxtaposes relatively old Proterozoic basement rocks in the north against relatively young rocks in the south, thus suggesting a similar configuration and kinematics as along the Kinnhøgda–Daudbjørnpynten fault zone in Storfjorden and the northeastern Norwegian Barents Sea. Moreover, von Gosen and Piepjohn (2001) and Bergh and Grogan (2003) reported that Devonian–Mississippian sedimentary successions and Cenozoic fold structures (e.g., Hyrnefjellet Anticline) are offset sinistrally by a few kilometers in Hornsund. Thus, we propose that the Vimsodden–Kosibapasset Shear Zone extends into Hornsund and represents the westwards continuation of the Kinnhøgda–Daudbjørnpynten fault zone. This suggests a minimum extent of 400–450 kilometers for this thrust system (Figure 1b–c and Figure 5a–c).

Timing of formation of major NNE-dipping thrust systems and N–S-trending folds

NNE-dipping thrust systems

The several-kilometer thickness and hundreds–thousands of kilometers along-strike extent of NNE-dipping thrust systems in central–eastern Spitsbergen, Storfjorden, and the northwestern and northeastern Norwegian Barents Sea suggest that they formed during a major contractional tectonic event. The overall WNW–ESE trend and the consistent north-northeastwards dip and top-SSW sense of shear along the newly evidenced deep thrust systems preclude formation during the

Grenvillian, Caledonian, and Ellesmerian orogenies, and the Eurekan tectonic event. These tectonic events all involved dominantly E–W-oriented contraction and resulted in the formation of overall N–S- to NNE–SSW-trending fabrics, structures and deformation belts in Svalbard (i.e., sub-orthogonal to the newly identified thrust systems) such as the Atomfjella Antiform (Gee et al., 1994; Witt-Nilsson et al., 1998), the Vestfonna and Rijpdalen anticlines (Johansson et al., 2004; 2005; Dumais and Brönnér, 2020), the Dickson Land and Germaniahelvøya fold-thrust zones (McCann, 2000; Piepjohn, 2000; Dallmann and Piepjohn, 2020), and the West Spitsbergen Fold-and-Thrust Belt and related early Cenozoic structures in eastern Spitsbergen (Andresen et al., 1992; Haremo and Andresen, 1992; Dallmann et al., 1993), and NE–SW- to NNE–SSW-striking thrusts and folds in northern Norway (Sturt et al., 1978; Townsend, 1987; Roberts and Williams, 2013) and the southwestern Barents Sea (Gernigon et al., 2014).

A possible cause for the formation of the observed NNE-dipping thrust systems is the late Neoproterozoic Timanian Orogeny, which is well known onshore northwestern Russia (e.g., Kanin Peninsula, Timan Range and central Timan; Siedlecka and Roberts, 1995; Olovyanishnikov et al., 2000; Kostyuchenko et al., 2006) and northeastern Norway (Varanger Peninsula; Siedlecka and Siedlecki, 1967; Siedlecka, 1975; Roberts and Olovyanishnikov, 2004), and traces of which were recently found in southwestern Spitsbergen (Majka et al., 2008, 2012, 2014) and northern Greenland (Rosa et al., 2016; Estrada et al., 2018). The overall transport direction during this orogeny was directed towards the south-southwest and most thrust systems show NNE-dipping geometries (Olovyanishnikov et al., 2000; Kostyuchenko et al., 2006), e.g., the Timanian thrust front on the Varanger Peninsula in northeastern Norway (Trollfjorden–Komagelva Fault Zone; Siedlecka and Siedlecki, 1967; Siedlecka, 1975). In addition, the size of Timanian thrust systems in the Timan Range (e.g., Central Timan Fault) is comparable (≥ 3 –4 seconds TWT; Kostyuchenko et al., 2006 their figure 17) to that of thrust systems in the northern Norwegian Barents Sea and Svalbard (Figure 3a and c–d).

Thus, based on their overall WNW–ESE strike (Figure 1b–c), their vergence to the south-southwest (Figure 3a, c–d and f), their coincidence with gravimetric and magnetic highs (Figure 5a–c), their upward truncation by a major unconformity consistently throughout the study area (see top-Precambrian unconformity in Figure 3a–d), and the correlation of these NNE-dipping thrusts (via gravimetric and magnetic anomalies) to similarly striking and verging structures of comparable size (i.e., several seconds TWT thick) onshore–nearshore northwestern Russia and northern

Norway (Siedlecka, 1975; Siedlecka and Roberts, 1995; Olovyanishnikov et al., 2000; Roberts and Siedlecka, 2002; Gee and Pease, 2004; Kostyuchenko et al., 2006), NNE-dipping thrusts in the northern Norwegian Barents Sea, Storfjorden, and central–eastern Spitsbergen are interpreted as the western continuation of Timanian thrusts.

Timanian grain was recently identified in the northeastern Norwegian Barents Sea through interpretation of new seismic, magnetic and gravimetric datasets shown in Figure 5a–c (Klitzke et al., 2019). The alignment, coincident location, and matching geometries (e.g., curving E–W to NW–SE strike/trend and kilometer-wide NNE–SSW-trending anticline) between Timanian grain and structures mapped by Klitzke et al. (2019) and the major, NNE-dipping, top-SSW thrust systems described in central–eastern Spitsbergen, Storfjorden and the Norwegian Barents Sea (Figure 3a–f and supplement S2) further support a Timanian origin for the latter. Further evidence of relic Timanian structural grain as far as the Loppa High and Bjørnøya Basin are documented by previous magnetic studies and modelling (Marello et al., 2010). Moreover, seismic mapping suggests that Timanian thrust systems extend well into central Spitsbergen (Figure 3e–f and supplement S2c–d; Koehl, 2020a; Koehl et al., 2021 in review), and regional gravimetric and magnetic anomaly maps suggest that Timanian thrust systems might extend farther west to (north-) western Spitsbergen (Figure 5a–c).

Probable reasons as to why these major (hundreds–thousands of kilometers long) thrust systems were not identified before during fieldwork in Svalbard are their burial to high depth (> 1–2 seconds TWT in the study area, i.e., several kilometers below the surface; Figure 3a–f), and their strong overprinting by younger tectonic events like the Caledonian Orogeny in areas where they are exposed (e.g., Vimsodden–Kosibapasset Shear Zone in southwestern Spitsbergen; Faehnrich et al., 2020). Possible areas of interest for future studies include the western and northwestern parts of Spitsbergen where Caledonian and Eureka E–W contraction contributed to uplift and exhume deep basement rocks, and where Timanian rocks potentially crop out (e.g., Peucat et al., 1989).

N–S-trending folds

N–S-trending upright folds involve the NNE-dipping thrust systems (Figure 3b and e) and correlate (via gravimetric and magnetic anomalies) with major Caledonian folds in northeastern Spitsbergen and Nordaustlandet, like the Atomfjella Antiform (Gee et al., 1994; Witt-Nilsson et

al., 1998) and Rijpdalen Anticline (Johansson et al., 2004; 2005; Dumais and Brönnner, 2020), with Caledonian grain in the southern Norwegian Barents Sea (Gernigon and Brönnner, 2012; Gernigon et al., 2014), and with major NE–SW-trending Caledonian folds onshore northern Norway (Sturt et al., 1978; Townsend, 1987; Roberts and Williams, 2013). In addition, the width of the NE–SW- to N–S-trending gravimetric and magnetic anomalies associated with these folds increases up to 150 kilometers eastwards, i.e., away from the Caledonian collision zone (Figure 5a–c; Corfu et al., 2014; Gasser, 2014). Thus, N–S-trending folds in the northern Norwegian Barents Sea are interpreted as Caledonian regional folds in Precambrian–lower Paleozoic rocks. The relatively broader geometry of Caledonian folds away from the Caledonian collision zone (e.g., in the Russian Barents Sea) is inferred to be related to gentler fold geometries due to decreasing deformation intensity in this direction. This is further supported by relatively low grade Caledonian metamorphism in Franz Josef Land (Knudsen et al., 2019; see Figure 1a–b for location). By contrast, the presence of tighter Caledonian folds near the collision zone in the northern Norwegian Barents Sea (e.g., Figure 3b and e, and Atomfjella Antiform and Rijpdalen Anticline onshore; Gee et al., 1994; Witt-Nilsson et al., 1998; Johansson et al., 2004, 2005; Dumais and Brönnner, 2020) is associated with much narrower (20–50 kilometers wide) gravimetric and magnetic anomalies (Figure 5a–c). Note that the Atomfjella Antiform and Rijpdalen Anticline can be directly correlated with 20–50 kilometers wide, N–S-trending high gravimetric and magnetic anomalies (Figure 5a–c). Noteworthy, some of the NNE–SSW-trending folds and anomalies in the northernmost Norwegian Barents Sea may reflect a combination of Caledonian and superimposed early Cenozoic Eureka folding (e.g., Kairanov et al., 2018).

The interference of WNW–ESE- and N–S- to NNE–SSW-trending gravimetric highs, which are correlated to Timanian and Caledonian folds respectively, produces oval-shaped gravimetric and magnetic highs (Figure 5a). These relatively higher, oval-shaped gravimetric anomalies are interpreted to correspond to dome-shaped folds resulting from the interaction of Timanian and Caledonian folds involving refolding of WNW–ESE-trending Timanian folds during E–W Caledonian contraction. Field studies on the Varanger Peninsula in northern Norway and seismic studies of Timanian thrusts off northern Norway where the interaction of Timanian and Caledonian folds produced dome-shaped fold structures (Ramsay, 1962), e.g., like the Ragnarokk Anticline (Siedlecka and Siedlecki, 1971; Koehl, in prep.) also support this interpretation. Furthermore, Barrère et al. (2011) suggested that basins and faults in the southern Norwegian

Barents Sea are controlled by the interaction of Caledonian and Timanian structural grain, and Marell et al. (2010) argued that elbow-shaped magnetic anomalies reflect the interaction of Caledonian and Timanian structural grains in the Barents Sea, potentially as far west as the Loppa High and the Bjørnøya Basin.

Phanerozoic reactivation and overprinting of Timanian thrust systems

Caledonian reactivation and overprint

The geometry of the Kongsfjorden–Cowanodden and Kinnhøgda–Daudbjørnpynten fault zones in Nordmannsfonna (Figure 3e) and the northeastern Norwegian Barents Sea (Figure 3b; Klitzke et al., 2019), where they are folded into broad NNE-plunging upright anticlines and synclines suggests that these thrust systems were deformed after they accommodated top-SSW Timanian thrusting (Figure 6a and Figure 7a). In addition, subsidiary top-west kinematics (west-verging folds and top-west minor thrusts) suggest that these thrust systems were partly reactivated–overprinted during an episode of intense E–W contraction (Figure 6b and Figure 7b). However, west-dipping dykes crosscutting and gently east-dipping sedimentary strata overlying the eastern part of the folded Kongsfjorden–Cowanodden fault zone are only mildly folded, and upper Paleozoic sedimentary strata lie flat over folded and partly eroded Precambrian–lower Paleozoic rocks and the Kinnhøgda–Daudbjørnpynten fault zone, thus suggesting that these sedimentary strata and dykes were not involved in this episode of E–W contraction (Figure 3e).

A notable episode of E–W contraction in Svalbard is the Caledonian Orogeny in the early–mid Paleozoic, which resulted in the formation of west-verging thrusts and N–S-trending folds of comparable size (c. 15–25 kilometers wide) to those affecting the Kongsfjorden–Cowanodden and Kinnhøgda–Daudbjørnpynten fault zones in Nordmannsfonna and the northern Norwegian Barents Sea (Figure 3b and e; Klitzke et al., 2019, their figures 3–5), such as the Atomfjella Antiform in northeastern Spitsbergen (Gee et al., 1994; Witt-Nilsson et al., 1998; Lyberis and Manby, 1999) and the Rijpdalen Anticline in Nordaustlandet (Figure 1b). Since the NNE-plunging anticline in Nordmannsfonna does not affect overlying Pennsylvanian–Mesozoic sedimentary strata (Figure 3e), we propose that they formed during Caledonian contraction (Figure 7b). This is supported by the involvement of the top-Precambrian unconformity and underlying NNE-dipping thrusts in N–S- to NNE-SSW-trending folds, and by the truncation of these folds by the top-Silurian unconformity, which is overlapped by mildly deformed to flat-lying upper Paleozoic strata (Figure

3b and Figure 4f). Furthermore, structures with geometries comparable to NNE-plunging folds in the northern Barents Sea and Svalbard were observed in northern Norway. An example is the Ragnarokk Anticline, a dome-shaped fold structure along the Timanian front thrust on the Varanger Peninsula, which results from the re-folding of Timanian thrusts and folds into a NE–SW-trending Caledonian trend (Siedlecka and Siedlecki, 1971).

Further support of a Caledonian origin for upright NNE-plunging folds in eastern Spitsbergen, Storfjorden and the northern Norwegian Barents Sea is that these folds are relatively tight in the west, in Nordmannsfonna and the northwestern Barents Sea (Figure 3b and e), whereas they show gradually gentler and more open geometries in the east, i.e., away from the Caledonian collision zone (Figure 3b). This is also shown by the gradual eastwards broadening of regional gravimetric and magnetic anomalies correlated with Caledonian folds suggesting gentler fold geometries related to decreasing (Caledonian) deformation intensity in this direction (Figure 5a–c). This contrasts with the homogeneous intensity of deformation along NNE-dipping thrusts on seismic data and with the homogeneous width of related gravimetric–magnetic anomalies from west to east in Svalbard and the Barents Sea (Figure 3a–f and Figure 5a–c and supplement S2).

In Nordmannsfonna, the Caledonian origin of the major 15–20 kilometers wide anticline, and the truncation of overlying, gently east-dipping, mildly folded sedimentary strata and crosscutting west-dipping dykes by the base-Pennsylvanian unconformity suggest that these sedimentary strata and dykes are Devonian (–Mississippian?) in age (Figure 6c–d). This is supported by the presence of thick Devonian–Mississippian collapse deposits in adjacent areas of central–northern Spitsbergen (Cutbill et al., 1976; Murascov and Mokin, 1979; Aakvik, 1981; Gjølberg, 1983; Manby and Lyberis, 1992; Friend et al., 1997), and by Middle Devonian to Mississippian ages (395–327 Ma) for dykes in central–northern Spitsbergen (Evdokimov et al., 2006), northern Norway (Lippard and Prestvik, 1997; Guise and Roberts, 2002), and northwestern Russia (Roberts and Onstott, 1995).

The occurrence of a > 0.5 second (TWT) reverse offset of the folded Kongsfjorden–Cowanodden fault zone and the lack of offset of the Devonian (–Mississippian?) dykes across the Agardhbukta Fault indicate that the latter fault formed as a top-west thrust during the Caledonian Orogeny. At depth, the Agardhbukta Fault merges with the eastern flank of the folded Kongsfjorden–Cowanodden fault zone. This, together with the presence of minor, high-angle, top-west brittle thrusts within the Kongsfjorden–Cowanodden fault zone (Figure 3e), indicates that the

Agardhbukta Fault reactivated and/or overprinted the eastern portion of the Kongsfjorden–Cowanodden fault zone in Nordmannsfonna during Caledonian contraction (Figure 6b and Figure 7b). Depth conversion using seismic velocities from Gernigon et al. (2018) suggest that the Agardhbukta Fault offset the Kongsfjorden–Cowanodden fault zone by ca. 2.4–2.5 kilometers top-west during Caledonian contraction (Figure 3e and supplement S3g). These kinematics are consistent with field observation in eastern Spitsbergen by Piepjohn et al. (2019, their figure 17b). However, Piepjohn et al. (2019) also suggested a significant component of Mesozoic–Cenozoic, down-east normal movement, which was not identified in Nordmannsfonna. This suggests either along strike variation in the movement history of the Agardhbukta Fault, either that the fault mapped on seismic data in Nordmannsfonna does not correspond to the Agardhbukta Fault of Piepjohn et al. (2019).

Considering the presence of crustal-scale, NNE-dipping, hundreds (to thousands?) of kilometers long (Timanian) thrust systems extending from the Barents Sea (and possibly from onshore Russia) to central–eastern and southern Spitsbergen and the northwestern Norwegian Barents Sea (Figure 5a–c) prior to the onset of E–W-oriented Caledonian contraction, it is probable that such large structures would have (at least partially) been reactivated and/or overprinted during subsequent tectonic events if suitably oriented. Under E–W contraction, WNW–ESE-striking, dominantly NNE-dipping Timanian faults would be oriented at c. 30° to the direction of principal stress and, therefore, be suitable (according to Anderson’s stress model) to reactivate/be overprinted with sinistral strike-slip movements. Such kinematics were recorded along the Vimsodden–Kosibapasset Shear Zone in Wedel Jarlsberg Land (Mazur et al., 2009) and within Hornsund (von Gosen and Piepjohn, 2001).

However, recent ^{40}Ar – ^{39}Ar geochronological determinations on muscovite within this structure suggest that this structure formed during the Caledonian Orogeny (Faehnrich et al. 2020). Nonetheless, the same authors also obtained Timanian ages (600–540 Ma) for (initial) movements along minor shear zones nearby and parallel to the Vimsodden–Kosibapasset Shear Zone. Since this large shear zone must have represented a major preexisting zone of weakness when Caledonian contraction initiated, it is highly probable that it was preferentially chosen to reactivate instead of minor shear zones. Thus, the Caledonian ages obtained along the Vimsodden–Kosibapasset Shear Zone most likely reflect complete resetting of the geochronometer along the shear zone due to large amounts of Caledonian reactivation–overprinting, while minor nearby shear zones preserved traces

of initial Timanian deformation. This is also supported by observations in northern Norway suggesting that Timanian thrusts (e.g., Trollfjorden–Komagelva Fault Zone) were reactivated as major strike-slip faults during the Caledonian Orogeny (Roberts, 1972; Herrevold et al., 2009; Rice 2014). This interpretation reconciles the strong differences in dipping angle and depth between the Kinnhøgda–Daudbjørnpynnten fault zone and the Vimsodden–Kosibapasset Shear Zone. The former was located away from the Caledonian collision zone and essentially retained its initial, moderately NNE-dipping Timanian geometry and was deeply buried during the Phanerozoic, whereas the latter was intensely deformed, pushed into a sub-vertical position, and uplifted and exhumed to the surface because it was located near or within the Caledonian collision zone.

Devonian–Carboniferous normal overprint–reactivation

In Nordmannsfonna, the wedge shape of Devonian (–Mississippian?) sedimentary strata in the hanging wall of the Kongsfjorden–Cowanodden fault zone suggest that the eastern portion of this thrust was reactivated as a gently–moderately dipping extensional detachment (Figure 6c) and, thus, that Devonian (–Mississippian?) strata in this area represent analogs to collapse deposits in northern Spitsbergen. The intrusion of west-dipping Devonian (–Mississippian?) dykes orthogonal to the eastern portion of the thrust system, i.e., orthogonal to extensional movements along the inverted east-dipping portion of the thrust (Figure 3e and Figure 6d) also supports this interpretation. Similar relationships were inferred in northwestern Spitsbergen, where Devonian collapse sediments were deposited along a N–S-trending Precambrian basement ridge bounded by a gently dipping, extensional mylonitic detachment (Braathen et al., 2018).

In Sassenfjorden, Storfjorden and the northeastern Norwegian Barents Sea, listric brittle normal faults showing down-NNE offsets and syn-tectonic thickening within Devonian–Carboniferous (–Permian?) sedimentary strata merge at depth with the uppermost part of NNE-dipping Timanian thrust systems like the Kongsfjorden–Cowanodden fault zone (Figure 3a and d and supplement S2c). This indicates that Timanian thrust systems were used as preexisting zones of weakness during late–post-orogenic collapse of the Caledonides in the Devonian–Carboniferous (Figure 6c–e and Figure 7c).

The presence of the Kongsfjorden–Cowanodden fault zone in Storfjorden and below Edgeøya also explains the strong differences between the Paleozoic sedimentary successions penetrated by the Plurdalen-1 and Raddendalen-1 exploration wells (Bro and Shvarts, 1983;

Harland and Kelly, 1997). Notably, the Plurdalen-1 well penetrated (at least) ca. 1600 meters thick Devonian–Mississippian sedimentary rocks in the direct hanging wall of the Kongsfjorden–Cowanodden fault zone and related listric brittle overprints (Figure 3a), whereas the interpretation of Bro and Shvarts (1983) suggests that the Raddedalen-1 well encountered thin (90–290 meters thick) Mississippian strata overlying (> 2 kilometers) thick lower Paleozoic sedimentary rocks ca. 30 kilometers farther northeast, i.e., away from the Kongsfjorden–Cowanodden fault zone and related overprints. The presence of thick Devonian sedimentary strata in the direct hanging wall of listric overprints of the Kongsfjorden–Cowanodden fault zone further supports late–post-Caledonian extensional reactivation–overprinting of NNE-dipping Timanian thrusts.

In central Spitsbergen, recently identified Early Devonian–Mississippian normal faults formed along and overprinted–reactivated major NNE-dipping ductile (mylonitic) shear zones and fabrics in Billefjorden (Koehl et al., 2021 in review) and Sassenfjorden–Tempelfjorden (Koehl, 2020a). These show sizes, geometries and kinematics comparable to those of the Kongsfjorden–Cowanodden fault zone, and are, therefore, interpreted as the western continuation of this thrust system. The Devonian–Carboniferous extensional reactivation–overprinting of the Kongsfjorden–Cowanodden fault zone in central Spitsbergen explains the southward provenance of northwards prograding sedimentary rocks of the uppermost Silurian–Lower Devonian Siktefjellet and Red Bay groups and Wood Bay Formation and the enigmatic WNW–ESE trend of the southern boundary of the Devonian Graben in central–northern Spitsbergen (Gee and Moody-Stuart, 1966; Friend et al., 1966; Friend and Moody-Stuart, 1972; Murascov and Mokin, 1979; Friend et al., 1997; McCann, 2000; Dallmann and Piepjohn, 2020; Koehl et al., 2021 in review).

Mild Triassic overprint

The Kongsfjorden–Cowanodden fault zone and associated overprints align with WNW–ESE- to NW–SE-striking normal faults onshore southern and southwestern Edgeøya in Kvalpynten, Negerpynten, and Øhmanfjellet (Osmundsen et al., 2014; Ogata et al., 2018). These faults display both listric and steep planar geometries in cross-section and bound thickened syn-sedimentary growth strata in lowermost Upper Triassic sedimentary rocks of the Tschermakfjellet and De Geerdalen formations (Ogata et al., 2018; Smyrak-Sikora et al., 2020). The Norwegian Barents Sea and Svalbard are believed to have remained tectonically quiet throughout the Triassic apart from minor deep-rooted normal faulting in the northwestern Norwegian Barents Sea (Anell

et al., 2013) and Uralides-related contraction in the (south-) east (Müller et al., 2019). Hence, we propose that the progradation and accumulation of thick sedimentary deposits of the Triassic deltaic systems above the southeastward continuation of the Kongsfjorden–Cowanodden fault zone may have triggered minor tectonic adjustments resulting in the development of a system of small half-grabens over the thrust system. Alternatively or complementary, the deposition of thick Triassic deltaic systems may have locally accelerated compaction of sedimentary strata underlying the Tschermakjellet Formation in south- and southwest-Edgeøya, e.g., of the potential pre-Triassic syn-tectonic growth strata along the Kongsfjorden–Cowanodden fault zone, and, thus, facilitated the development of minor half-grabens within the Triassic succession along this thrust system.

Eurekan reactivation–overprint

In eastern Spitsbergen, the Agardhbukta Fault segment of the Lomfjorden Fault Zone truncates the Kongsfjorden–Cowanodden fault zone with a major, > 0.5 second (TWT) top-west reverse offset (Figure 3e). The Agardhbukta fault also mildly folds Pennsylvanian–Mesozoic sedimentary rocks and Cretaceous sills into a gentle upright (fault-propagation) fold with no major offset (Figure 6f–g), which is supported by onshore field observations in eastern and northeastern Spitsbergen (Piepjohn et al., 2019). Mild folding of Mesozoic sedimentary rocks and of Cretaceous intrusions indicates that the Agardhbukta Fault was most likely mildly reactivated as a top-west thrust during the early Cenozoic Eurekan tectonic event (Figure 6g and Figure 7d).

Seismic data show that high-angle listric Devonian–Carboniferous normal faults were mildly reactivated as reverse faults that propagated upwards and gently folded adjacent upper Paleozoic–Mesozoic (–Cenozoic?) sedimentary strata in the northwestern Norwegian Barents Sea, Storfjorden and central–eastern Spitsbergen (Figure 3a–c and supplement S2), but not in the northeastern Norwegian Barents Sea (Figure 3d). Since normal faults were not inverted in the east, it is probable that inversion of these faults in central–eastern Spitsbergen, Storfjorden and the northwestern Norwegian Barents Sea first occurred during the Eurekan tectonic event in the early Cenozoic, when Greenland collided with western Spitsbergen (Figure 7d). This is also supported by the gently folded character of Devonian–Mesozoic (–Cenozoic?) sedimentary successions in the west (Figure 3a and c), whereas these successions are essentially flat-lying (i.e., undeformed) in the east (Figure 3b and d). Nevertheless, folding of the seafloor reflection in Storfjorden and the

northwestern Norwegian Barents Sea suggests ongoing contractional deformation along several of these faults in the northwestern Norwegian Barents Sea and Storfjorden (Figure 3a–c).

Major, top-SSW mylonitic shear zones in Sassenfjorden–Tempelfjorden and Billefjorden display early Cenozoic overprints including top-SSW duplexes in uppermost Devonian–Mississippian coals of the Billefjorden Group acting as a partial décollement along a major basement-seated listric brittle fault (Koehl, 2020a; supplement S2) and NNE-dipping brittle faults offsetting the east-dipping Billefjorden Fault Zone by hundreds of meters to several kilometers left-laterally (Koehl et al., 2021 in review). Thus, the correlation of the Kongsfjorden–Cowanodden fault zone with these top-SSW mylonitic shear zones in Sassenfjorden–Tempelfjorden and Billefjorden (see Figure 1c for location) supports reactivation–overprinting of major NNE-dipping Timanian thrust systems as top-SSW, sinistral-reverse, oblique-slip thrusts in the early Cenozoic Eurekan tectonic event. Such correlation explains the NW–SE trend and the location of the northeastern boundary of the Central Tertiary Basin, which terminates just southwest of Sassenfjorden and Sassendalen in central Spitsbergen (Figure 1b–c). It also explains the dominance of NW–SE- to WNW–ESE-striking faults within Cenozoic deposits of the Central Tertiary Basin (Livshits, 1965a), and the northwestwards provenance (Petersen et al., 2016) and northwards thinning of sediments deposited in the basin (Livshits, 1965b), which were probably sourced from uplifted areas in the hanging wall of the reactivated–overprinted thrust.

Noteworthy, Livshits (1965a) argued that the Central Tertiary Basin was bounded to the north by a major WNW–ESE-striking fault extending from Kongsfjorden to southern Billefjorden–Sassenfjorden where the NNE-dipping Kongsfjorden–Cowanodden fault zone was mapped (present study; supplement S2). This indicates that the Kongsfjorden–Cowanodden fault zone might extend west of Billefjorden and Sassenfjorden, potentially until Kongsfjorden (see Figure 1c for location). Should it be the case, the Kongsfjorden–Cowanodden fault zone would coincide with a major terrane boundary in Svalbard, which was speculated to correspond to one or more regional WNW–ESE- to N–S-striking faults in earlier works, e.g., Kongsvegen Fault and Lapsdalen Thrust (Harland and Horsfield, 1974), Kongsvegen Fault Zone and/or Central–West Fault Zone (Harland and Wright, 1979), and Kongsfjorden–Hansbreen Fault Zone (Harland et al., 1993). The presence of a major, (inherited Timanian) NNE-dipping, basement-seated fault zone in this area would explain the observed strong differences between Precambrian basement rocks in Svalbard’s northwestern and southwestern terranes.

In southern Spitsbergen, von Gosen and Piepjohn (2001) and Bergh and Grogan (2003) suggested the presence of a WNW–ESE-striking, sinistral-reverse strike-slip fault in Hornsund based on a one-kilometer left-lateral offset of Devonian–Carboniferous sedimentary successions and of the early Cenozoic Hyrnefjellet Anticline across the fjord. This fault is part of the Kinnhøgda–Daudbjørnpynnten fault zone and was most likely reactivated–overprinted during Eureka contraction–transpression in the early Cenozoic.

Present day tectonism

Seismic data show that the seafloor reflection is folded and/or offset in a reverse fashion by high-angle brittle faults merging at depth with interpreted Timanian thrust systems in Storfjorden and just north of Bjørnøya in the northwestern Norwegian Barents (Figure 3a and c, and Figure 4h). This indicates that some of the Timanian thrust systems are still active at present and are reactivated/overprinted by reverse faults (Figure 7e). A potential explanation for ongoing reactivation–overprinting is transfer of extensional tectonic stress in the Fram Strait as ridge-push tectonism through Spitsbergen and Storfjorden.

Implication for plate tectonics reconstructions of the Barents Sea and Svalbard in the late Neoproterozoic–Paleozoic

The presence of hundreds to thousands of kilometers long Timanian faults throughout the northern Norwegian Barents Sea and central and southwestern (and possibly northwestern?) Spitsbergen indicates that the northwestern, northeastern and southwestern basement terranes of the Svalbard Archipelago were most likely already accreted together and attached to the Barents Sea, northern Norway and northwestern Russia in the late Neoproterozoic (ca. 600 Ma). Svalbard’s three terranes were previously thought to have been juxtaposed during the Caledonian and Ellesmerian orogenies through hundreds–thousands of kilometers of displacement along presumed thousands of kilometers long N–S-striking strike-slip faults like the Billefjorden Fault Zone (Harland, 1969; Harland et al. 1992, Labrousse et al., 2008; Figure 2). The presence of laterally continuous (undisrupted), hundreds–thousands of kilometers long, Timanian thrust systems from southwestern and central Spitsbergen to the northern Norwegian and Russian Barents Sea clearly shows that this is not possible (Figure 8).

The continuous character of these thrust systems from potentially as far as onshore northwestern Russia through the Barents Sea and Svalbard precludes any major strike-slip displacement along N–S-striking faults such as the Billefjorden Fault Zone and Lomfjorden Fault Zone (as proposed by Harland et al., 1974, 1992; Labrousse et al., 2008; Figure 2) and any hard-linked connection between these faults in Svalbard and analogous, NE–SW-striking faults in Scotland in the Phanerozoic (as proposed by Harland, 1969). Instead, the present work suggests that the crust constituting the Barents Sea and the northeastern and southwestern basement terranes of Svalbard should be included as part of Baltica in future Arctic plate tectonics reconstructions for the late Neoproterozoic–Paleozoic period (i.e., until ca. 600 Ma; Figure 8). It also suggests that the Caledonian suture zone, previously inferred to lie east of Svalbard in the Barents Sea (e.g., Gee and Teben'kov, 2004; Breivik et al., 2005; Barrère et al., 2011; Knudsen et al., 2019) may be located west of the presently described Timanian thrust systems, i.e., probably west of or in western Spitsbergen where Caledonian blueschist and eclogite metamorphism has been recorded in Precambrian basement rocks (Horsfield, 1972; Dallmeyer et al., 1990a; Ohta et al., 1995; Kosminska et al., 2014).

Conclusions

- 1) Seismic data in the northern Norwegian Barents Sea and Svalbard reveal the existence of several systems of hundreds–thousands of kilometers long, several kilometers thick, top-SSW thrusts comprised of brittle–ductile thrusts, mylonitic shear zones and associated SSW-verging folds that appear to extend from onshore northwestern Russia to the northern Norwegian Barents Sea and to central and southwestern Spitsbergen. A notable structure is the Kongsfjorden–Cowanodden fault zone in Svalbard and the Norwegian Barents Sea, which likely merges with the Baidaratsky fault zone in the Russian Barents Sea and southern Novaya Zemlya. We interpret these thrust systems as being related to the Neoproterozoic Timanian Orogeny.
- 2) In the east (away from the Caledonian collision zone), these Timanian thrusts systems were folded into NNE-plunging folds, offset, and reactivated as and/or overprinted by top-west, oblique-slip sinistral-reverse, brittle–ductile thrusts during subsequent Caledonian (e.g., Agardhbukta Fault segment of the Lomfjorden Fault Zone) and, possibly, during Eurekan contraction, and are deeply buried. By contrast, in the west (near or within the Caledonian

collision zone), Timanian thrusts were intensely deformed, pushed into sub-vertical positions, extensively overprinted, and exhumed to the surface.

- 3) In eastern Spitsbergen, a major NNE-dipping Timanian thrust system, the Kongsfjorden–Cowanodden fault zone, is crosscut by a swarm of Devonian (–Mississippian?) dykes that intruded contemporaneous sedimentary strata deposited during extensional reactivation of the eastern portion of the thrust system as a low-angle extensional detachment during late–post-Caledonian collapse.
- 4) Timanian thrust systems were overprinted by NNE-dipping, brittle normal faults in the late Paleozoic during the collapse of the Caledonides and/or subsequent rifting in the Devonian–Carboniferous.
- 5) Timanian thrust systems and associated Caledonian and Devonian–Carboniferous brittle overprints (e.g., Agardhbukta Fault) in the northwestern Norwegian Barents Sea and Svalbard were mildly reactivated during the early Cenozoic Eurekan tectonic event, which resulted in minor folding and minor reverse offsets of Devonian–Mesozoic sedimentary strata and intrusions. Timanian thrusts and related overprints in the northeastern Norwegian Barents Sea were not reactivated during the Eurekan tectonic event.
- 6) The presence of hundreds–thousands of kilometers long Timanian thrust systems may suggest that the Barents Sea and Svalbard’s three basement terranes were already attached to northern Norway and northwestern Russia in the late Neoproterozoic (ca. 600 Ma). If correct, a Timanian origin for these structures would preclude any major strike-slip movements along major N–S-striking faults like the Billefjorden and Lomfjorden fault zones in the Phanerozoic, and imply that the Caledonian suture zone is located west of or in western Spitsbergen.

Acknowledgements

The present study was supported by the Research Council of Norway, the Tromsø Research Foundation, and six industry partners through the Research Centre for Arctic Petroleum Exploration (ARCEX; grant number 228107), the SEAMSTRESS project (grant number 287865), and the Centre for Earth Evolution and Dynamics (CEED; grant number 223272). We thank the Norwegian Petroleum Directorate and the Federal Institute for Geosciences and Natural Resources (BGR) for granting access and allowing publication of seismic, magnetic and gravimetric data in

1111 Svalbard and the Norwegian Barents Sea. Prof. Steffen Bergh, Dr. Winfried Dallmann, Prof. Jiri
1112 Konopasek, Assoc. Prof. Mélanie Forien, Dr. Kate Waghorn (UiT The Arctic University of Norway
1113 in Tromsø), Dr. Peter Klitzke (Federal Institute for Geosciences and Natural Resources –
1114 Germany), Anna Dichiarante (Norway Seismic Array), Rune Matningsdal (Norwegian Petroleum
1115 Directorate), and Prof. Carmen Gaina (Centre for Earth Evolution and Dynamics, University of
1116 Oslo) are thanked for fruitful discussion.

1117

1118 **Data availability**

1119 For high-resolution versions of the figures and supplements, the reader is referred to the
1120 Open Access data repository DataverseNO (doi.org/10.18710/CE8RQH).

1121

1122 **References**

- 1123 Aakvik, R.: Fasies analyse av Undre Karbonske kullførende sedimenter, Billefjorden, Spitsbergen,
1124 Ph.D. Thesis, University of Bergen, Bergen, Norway, 219 pp., 1981.
- 1125 Andresen, A., Haremo, P., Swensson, E. and Bergh, S. G.: Structural geology around the southern
1126 termination of the Lomfjorden Fault Complex, Agardhdalen, east Spitsbergen, Norsk Geol.
1127 Tidsskr., 72, 83–91, 1992.
- 1128 Anell, I., Braathen, A., Olaussen, S. and Osmundsen, P. T.: Evidence of faulting contradicts a
1129 quiescent northern Barents Shelf during the Triassic, First Break, 31, 67–76, 2013.
- 1130 Anell, I. M., Braathen, A. and Olaussen, S.: Regional constraints of the Sørkapp Basin: A
1131 Carboniferous relic or a Cretaceous depression, Mar. Petrol. Geol., 54, 123–138, 2014.
- 1132 Anell, I. M., Faleide, J. I. and Braathen, A.: Regional tectono-sedimentary development of the
1133 highs and basins of the northwestern Barents Shelf, Norsk Geologisk Tidsskrift, 96, 1, 27–
1134 41, 2016.
- 1135 Arbaret, L. and Burg, J.-P.: Complex flow in lowest crustal, anastomosing mylonites: Strain
1136 gradients in a Kohistan gabbro, northern Pakistan, J. Geophys. Res., 108, 2467, 2003.
- 1137 Barrère, C., Ebbing, J. and Gernigon, L.: Offshore prolongation of Caledonian structures and
1138 basement characterization in the western Barents Sea from geophysical modelling,
1139 Tectonophys., 470, 71–88, 2009.

1140 Barrère, C., Ebbing, J. and Gernigon, L.: 3-D density and magnetic crustal characterization of the
 1141 southwestern Barents Shelf: implications for the offshore prolongation of the Norwegian
 1142 Caledonides, *Geophys. J. Int.*, 184, 1147–1166, 2011.

1143 Boyer, S. E. and Elliott, D.: Thrust Systems, *AAPG Bulletin*, 66, 9, 1196–1230, 1982.

1144 Braathen, A., Bælum, K., Maher Jr., H. D. and Buckley, S. J.: Growth of extensional faults and
 1145 folds during deposition of an evaporite-dominated half-graben basin; the Carboniferous
 1146 Billefjorden Trough, Svalbard, *Norsk Geol. Tidsskr.*, 91, 137–160, 2011.

1147 Braathen, A., Osmundsen, P. T., Maher, H. and Ganerød, M.: The Keisarhjelmen detachment
 1148 records Silurian–Devonian extensional collapse in Northern Svalbard, *Terra Nova*, 30, 34–
 1149 39, 2018.

1150 Breivik, A. J., Mjelde, R., Grogan, P., Shimamura, H., Murai, Y. and Nishimura, Y.: Caledonide
 1151 development offshore–onshore Svalbard based on ocean bottom seismometer, conventional
 1152 seismic, and potential field data, *Tectonophys.*, 401, 79–117, 2005.

1153 Bro, E. G. and Shvarts, V. H.: Processing results from drill hole Raddedalen-1, Edge Island,
 1154 Spitzbergen Archipelago, All-Russian Research Institute for Geology and Mineral
 1155 Resources of the World Ocean, St. Petersburg, Pangaea, Report 5750, 1983.

1156 Cawood, P. A., McCausland, P. J. A. and Dunning, G. R.: Opening Iapetus: Constraints from the
 1157 Laurentian margin in Newfoundland, *GSA Bull.*, 113, 4, 443–453, 2001.

1158 Chalmers, J. A. and Pulvertaft, T. C. R.: Development of the continental margins of the Labrador
 1159 Sea: a review, in: *Non-Volcanic Rifting of Continental Margins: A Comparison of*
 1160 *Evidence from Land and Sea*, edited by: Wilson, R. C. L., Taylor, R. B. and Froitzheim,
 1161 N., *Geol. Soc. London, Spec. Publi.*, 187, 77–105, 2001.

1162 Cocks, L. R. M. and Torsvik, T. H.: Baltica from the late Precambrian to mid-Palaeozoic times:
 1163 The gain and loss of a terrane’s identity, *Earth-Sci. Rev.*, 72, 39–66, 2005.

1164 Colombu, S., Cruciani, G., Fancello, D., Franceschelli, M. and Musumeci, G.: Petrophysical
 1165 properties of a granite-protomylonite-ultramylonite sequence: insight from the Monte
 1166 Grighini shear zone, central Sardinia, Italy, *Eur. J. Mineral*, 27, 471–486, 2015.

1167 Corfu, F., Andersen, T. B. and Gasser, D.: The Scandinavian Caledonides: main features,
 1168 conceptual advances and critical questions, in: *New Perspectives on the Caledonides of*
 1169 *Scandinavia and Related Areas*, edited by: Corfu, F., Gasser, D. and Chew, D. M., *Geol.*
 1170 *Soc., London, Spec. Publi.*, 390, 9–43, 2014.

- 1171 Cutbill, J. L. and Challinor, A.: Revision of the Stratigraphical Scheme for the Carboniferous and
1172 Permian of Spitsbergen and Bjørnøya, *Geol. Mag.*, 102, 418–439, 1965.
- 1173 Cutbill, J. L., Henderson, W. G. and Wright, N. J. R.: The Billefjorden Group (Early Carboniferous)
1174 of central Spitsbergen, *Norsk Polarinst. Skr.*, 164, 57–89, 1976.
- 1175 Dallmann, W. K.: *Geoscience Atlas of Svalbard*, Norsk Polarinstitut, Tromsø, Norway,
1176 Rapportserie nr. 148, 2015.
- 1177 Dallmann, W. K. and Krasil'scikov, A. A.: Geological map of Svalbard 1:50,000, sheet D20G
1178 Bjørnøya, *Norsk Polarinst. Temakart*, 27, 1996.
- 1179 Dallmann, W. K. and Piepjohn, K.: The structure of the Old Red Sandstone and the Svalbardian
1180 Orogenic Event (Ellesmerian Orogeny) in Svalbard, *Norg. Geol. Unders. B., Spec. Publi.*,
1181 15, 106 pp., 2020.
- 1182 Dallmeyer, R. D., Peucat, J. J., Hirajima, T. and Ohta, Y.: Tectonothermal chronology within a
1183 blueschist–eclogite complex, west-central Spitsbergen, Svalbard: Evidence from $^{40}\text{Ar}/^{39}\text{Ar}$
1184 and Rb–Sr mineral ages, *Lithos*, 24, 291–304, 1990a.
- 1185 Dallmeyer, R. D., Peucat, J. J. and Ohta, Y.: Tectonothermal evolution of contrasting metamorphic
1186 complexes in northwest Spitsbergen (Biskayerhalvøya): Evidence from $^{40}\text{Ar}/^{39}\text{Ar}$ and Rb-
1187 Sr mineral ages, *GSA Bull.*, 102, 653–663, 1990b.
- 1188 Dewey, J. F. and Strachan, R. A.: Changing Silurian–Devonian relative plate motion in the
1189 Caledonides: sinistral transpression to sinistral transtension, *J. Geol. Soc., London*, 160,
1190 219–229, 2003.
- 1191 Drachev, S. S.: Fold belts and sedimentary basins of the Eurasian Arctic, *Arktos*, 2:21, 2016.
- 1192 Drachev, S. S., Malyshev, N. A. and Nikishin, A. M.: Tectonic history and petroleum geology of
1193 the Russian Arctic Shelves: an overview, *Petrol. Geol. Conf. series*, 7, 591–619, 2010.
- 1194 Dumais, M.-A. and Brönnert, M.: Revisiting Austfonna, Svalbard, with potential field methods – a
1195 new characterization of the bed topography and its physical properties, *The Cryosphere*,
1196 14, 183–197, 2020.
- 1197 Eldholm, O. and Ewing, J.: Marine Geophysical Survey in the Southwestern Barents Sea, *J.*
1198 *Geophys. Res.*, 76, 17, 3832–3841, 1971.
- 1199 Engen, Ø., Faleide, J. I. and Dyreng, T. K.: Opening of the Fram Strait gateway: A review of plate
1200 tectonic constraints, *Tectonophys.*, 450, 51–69, 2008.

- 1201 Estrada, S., Tessensohn, F. and Sonntag, B.-L.: A Timanian island-arc fragment in North
1202 Greenland: The Midtkap igneous suite, *J. Geodyn.*, 118, 140–153, 2018.
- 1203 Faehnrich, K., Majka, J., Schneider, D., Mazur, S., Manecki, M., Ziemniak, G., Wala, V. T. and
1204 Strauss, J. V.: Geochronological constraints on Caledonian strike-slip displacement in
1205 Svalbard, with implications for the evolution of the Arctic, *Terra Nova*, 2020, 32, 290–299.
- 1206 Fortey, R. A. and Bruton, D. L.: Lower Ordovician trilobites of the Kirtonryggen Formation,
1207 Spitsbergen, *ossils and Strata*, 59, Wiley Blackwell, 120 pp., 2013.
- 1208 Fountain, D. M., Hurich, C. A. and Smithson, S. B.: Seismic relectivity of mylonite zones in the
1209 crust, *Geology*, 12, 195–198, 1984.
- 1210 Friend, P. F. and Moody-Stuart, M.: Sedimentation of the Wood Bay Formation (Devonian) of
1211 Spitsbergen: Regional analysis of a late orogenic basin, *Norsk Polarinst. Skr.*, 157, 80 pp.,
1212 1972.
- 1213 Friend, P. F., Heintz, N. and Moody-Stuart, M.: New unit terms for the Devonian of Spitsbergen
1214 and a new stratigraphical scheme for the Wood Bay Formation, *Polarinst. Årbok*, 1965, 59–
1215 64, 1966.
- 1216 Friend, P. F., Harland, W. B., Rogers, D. A., Snape, I. and Thornley, R. S.: Late Silurian and Early
1217 Devonian stratigraphy and probable strike-slip tectonics in northwestern Spitsbergen, *Geol.*
1218 *Mag.*, 134, 4, 459–479, 1997.
- 1219 Gasser, D.: The Caledonides of Greenland, Svalbard and other Arctic areas: status of research and
1220 open questions, in: *New Perspectives on the Caledonides of Scandinavia and Related Areas*,
1221 edited by: Corfu, F., Gasser, D. and Chew, D. M., *Geol. Soc., London, Spec. Publi.*, 390,
1222 93–129, 2014.
- 1223 Gee, D. G. and Moody-Stuart, M.: The base of the Old Red Sandstone in central north Haakon VII
1224 Land, Vestspitsbergen, *Polarinst. Årbok*, 1964, 57–68, 1966.
- 1225 Gee, D. G. and Pease, V.: The Neoproterozoic Timanide Orogen of eastern Baltica: introduction,
1226 in: *The Neoproterozoic Timanide Orogen of eastern Baltica*, edited by: Gee, D. G. and
1227 Pease, V., *Geol. Soc. London, Mem.*, 30, 1–3, 2004.
- 1228 Gee, D. G. and Teben'kov, A. M.: Svalbard: a fragment of the Laurentian margin, in: *The*
1229 *Neoproterozoic Timanide Orogen of eastern Baltica*, edited by: Gee, D. G. and Pease, V.,
1230 *Geol. Soc. London, Mem.*, 30, 191–206, 2004.

- 1231 Gee, D. G., Björklund, L. and Stølen, L.-K.: Early Proterozoic basement in Ny Friesland–
1232 implications for the Caledonian tectonics of Svalbard, *Tectonophys.*, 231, 171–182, 1994.
- 1233 Gee, D. G., Fossen, H., Henriksen, N. and Higgins, A. K.: From the Early Paleozoic Platforms of
1234 Baltica and Laurentia to the Caledonide Orogen of Scandinavia and Greenland, *Episodes*,
1235 31, 1, 44–51, 2008.
- 1236 Gernigon, L. and Brönnner, M.: Late Palaeozoic architecture and evolution of the southwestern
1237 Barents Sea: insights from a new generation of aeromagnetic data, *J. Geol. Soc., London*,
1238 169, 449–459, 2012.
- 1239 Gernigon, L., Brönnner, M., Roberts, D., Olesen, O., Nasuti, A. and Yamasaki, T.: Crustal and basin
1240 evolution of the southwestern Barents Sea: From Caledonian orogeny to continental
1241 breakup, *Tectonics*, 33, 347–373, 2014.
- 1242 Gernigon, L., Brönnner, M., Dumais, M.-A., Gradmann, S., Grønlie, A., Nasuti, A. and Roberts, D.:
1243 Basement inheritance and salt structures in the SE Barents Sea: Insights from new potential
1244 field data, *J. Geodyn.*, 119, 82–106, 2018.
- 1245 Griffin, W. L., Nikolic, N., O'Reilly, S. Y. and Pearson, N. J.: Coupling, decoupling and
1246 metasomatism: Evolution of crust–mantle relationships beneath NW Spitsbergen, *Lithos*,
1247 149, 115–135, 2012.
- 1248 Gudlaugsson, S. T., Faleide, J. I., Johansen, S. E. and Breivik, A. J.: Late Palaeozoic structural
1249 development of the South-western Barents Sea. *Mar. Petrol. Geol.*, 15, 73–102, 1998.
- 1250 Haremo, P. and Andresen, A.: Tertiary décollements thrusting and inversion structures along
1251 Billefjorden and Lomfjorden Fault Zones, East Central Spitsbergen, in: *Structural and*
1252 *Tectonic Modelling and its Application to Petroleum Geology*, edited by: Larsen, R. M.,
1253 Brekke, H., Larsen, B. T. and Talleraas, E., Norwegian Petroleum Society (NPF) Special
1254 Publications, 1, 481–494, 1992.
- 1255 Harland, W. B.: Contribution of Spitsbergen to understanding of tectonic evolution of North
1256 Atlantic region, *AAPG Memoirs*, 12, 817–851, 1969.
- 1257 Harland, W. B. and Horsfield, W. T.: West Spitsbergen Orogen, in: *Mesozoic–Cenozoic Orogenic*
1258 *Belts, data for Orogenic Studies*, *J. Geol. Soc. London, Spec. Publi.*, 4, 747–755, 1974.
- 1259 Harland, W. B. and Kelly, S. R. A.: Eastern Svalbard Platform, in: *Geology of Svalbard*, edited by:
1260 Harland, W. B., *Geol. Soc. London, Mem.*, 17, 521 pp., 1997.

- 1261 Harland, W. B. and Wright, N. J. R.: Alternative hypothesis for the pre-Carboniferous evolution of
1262 Svalbard, Norsk Polarinst. Skr., 167, 89–117, 1979.
- 1263 Harland, W. B., Cutbill, L. J., Friend, P. F., Gobbett, D. J., Holliday, D. W., Maton, P. I., Parker,
1264 J. R. and Wallis, R. H.: The Billefjorden Fault Zone, Spitsbergen – the long history of a
1265 major tectonic lineament, Norsk Polarinst. Skr., 161, 1–72, 1974.
- 1266 Harland, W. B., Scott, R. A., Auckland, K. A. and Snape, I.: The Ny Friesland Orogen, Spitsbergen,
1267 Geol. Mag., 129, 6, 679–708, 1992.
- 1268 Harland, W. B., Hambrey, M. J. and Waddams, P.: Vendian geology of Svalbard, Norsk Polarinst.
1269 Skri., 193, 152 pp., 1993.
- 1270 Hassaan, M., Faleide, J. I., Gabrielsen, R. H. and Tsikalas, F.: Carboniferous graben structures,
1271 evaporite accumulations and tectonic inversion in the southeastern Norwegian Barents Sea,
1272 Mar. Petrol. Geol., 112, 104038, 2020a.
- 1273 Hassaan, M., Faleide, J. I., Gabrielsen, R. H. and Tsikalas, F.: Architecture of the evaporite
1274 accumulation and salt structures dynamics in Tiddlybanken Basin, southeastern Norwegian
1275 Barents Sea, Basin Res., 33, 91–117, 2020b.
- 1276 Herrevold, T., Gabrielsen, R. H. and Roberts, D.: Structural geology of the southeastern part of the
1277 Trollfjorden-Komagelva Fault Zone, Varanger Peninsula, Finnmark, North Norway,
1278 Norwegian Journal of Geology, 89, 305–325, 2009.
- 1279 Horsfield, W. T.: Glaucophane schists of Caledonian age from Spitsbergen, Geol. Mag., 109, 1,
1280 29–36, 1972.
- 1281 Hurich, C. A., Smithson, S. B., Fountain, D. M. and Humphreys, M. C.: Seismic evidence of
1282 mylonite reflectivity and deep structure in the Kettle dome metamorphic core complex,
1283 Washington, Geology, 13, 577–580, 1985.
- 1284 Jakobsson, M., Mayer, L., Coackley, B., Dowdeswell, J. A., Forbes, S., Fridman, B., Hodnesdal,
1285 H., Noormets, R., Pedersen, R., Rebesco, M., Schenke, H. W., Zarayskaya, Y., Accettella,
1286 D., Armstrong, A., Anderson, R. M., Bienhoff, P., Camerlenghi, A., Church, I., Edwards,
1287 M., Gardner, J. V., Hall, J. K., Hell, B., Hestvik, O., Kristoffersen, Y., Marcussen, C.,
1288 Mohammad, R., Mosher, D., Nghiem, S. V., Pedrosa, M. T., Travaglini, P. G., and
1289 Weatherall, P.: The International Bathymetric Chart of the Arctic Ocean (IBCAO) Version
1290 3.0, Geophys. Res. Lett., 39, L12609, <https://doi.org/10.1029/2012GL052219>, 2012.

1291 Johansen, S. E., Ostistý, B. K., Birkeland, Ø., Fedorovsky, Y. F., Martirosjan, V. N., Bruun
1292 Christensen, O., Cheredeev, S. I., Ignatenko, E. A. and Margulis, L. S.: Hydrocarbon
1293 potential in the Barents Sea region: play distribution and potential, in: Arctic Geology and
1294 Petroleum Potential, edited by: Vorren, T. O., Bergsager, E., Dahl-Stamnes, Ø. A., Holter,
1295 E., Johansen, B., Lie, E. and Lund, T. B., NPF Spec. Publi., 2, 273–320, Elsevier,
1296 Amsterdam, 1992.

1297 Johansson, Å., Larionov, A. N., Gee, D. G., Ohta, Y., Tebenkov, A. M. and Sandelin, S.:
1298 Grenvillian and Caledonian tectono-magmatic activity in northeasternmost Svalbard, in:
1299 The Neoproterozoic Timanide Orogen of Eastern Baltica, edited by: Gee, D. G. and Pease,
1300 V., Geol. Soc. London Memoirs, 30, 207–232, 2004.

1301 Johansson, Å., Gee, D. G., Larionov, A. N., Ohta, Y. and Tebenkov, A. M.: Grenvillian and
1302 Caledonian evolution of eastern Svalbard – a tale of two orogenies, *Terra Nova*, 17, 317–
1303 325, 2005.

1304 Kairanov, B., Escalona, A., Mordascova, A., Sliwiska, K. and Suslova, A.: Early Cretaceous
1305 tectonostratigraphy evolution of the north central Barents Sea, *J. Geodyn.*, 119, 183–198,
1306 2018.

1307 Klitzke, P., Franke, D., Ehrhardt, A., Lutz, R., Reinhardt, L., Heyde, I. and Faleide, J. I.: The
1308 Palaeozoic Evolution of the Olga Basin Region, Northern Barents Sea: A Link to the
1309 Timanian Orogeny, *Geochem., Geophys., Geosy.*, 20, 614–629, 2019.

1310 Knudsen, C., Gee, D. G., Sherlock, S. C. and Yu, L.: Caledonian metamorphism of metasediments
1311 from Franz Josef Land, *GFF*, 141, 295–307, 2019.

1312 Koehl, J.-B. P.: Early Cenozoic Eurekan strain partitioning and decoupling in central Spitsbergen,
1313 Svalbard, *Solid Earth*, 12, 1025–1049, 2020a.

1314 Koehl, J.-B. P.: Impact of Timanian thrusts on the Phanerozoic tectonic history of Svalbard,
1315 Keynote lecture, EGU General Assembly, May 3rd–8th 2020, Vienna, Austria, 2020b.

1316 Koehl, J.-B. P. and Muñoz-Barrera, J. M.: From widespread Mississippian to localized
1317 Pennsylvanian extension in central Spitsbergen, Svalbard, *Solid Earth*, 9, 1535–1558, 2018.

1318 Koehl, J.-B. P., Bergh, S. G., Henningsen, T. and Faleide, J. I.: Middle to Late Devonian–
1319 Carboniferous collapse basins on the Finnmark Platform and in the southwesternmost
1320 Nordkapp basin, SW Barents Sea, *Solid Earth*, 9, 341–372, 2018.

- 1321 Koehl, J.-B. P., Bergh, S. G., Osmundsen, P. T., Redfield, T., Indrevær, K., Lea, H. and Bergø, E.:
 1322 Late Devonian–Carboniferous faulting and controlling structures and fabrics in NW
 1323 Finnmark, *Norw. J. Geol.*, 99, 3, 1–40, 2019.
- 1324 Koehl, J.-B. P., Allaart, L. and Noormets, R.: Devonian–Carboniferous collapse and segmentation
 1325 of the Billefjorden Trough, and Eurekan inversion–overprint and strain partitioning and
 1326 decoupling along inherited WNW–ESE-striking faults, in review, 2021.
- 1327 Korago, E. A., Kovaleva, G. N., Lopatin, B. G. and Orgo, V. V.: The Precambrian rocks of Novaya
 1328 Zemlya, in: *The Neoproterozoic Timanide Orogen of Eastern Baltica*, edited by: Gee, D.
 1329 G. and Pease, V., *Geol. Soc. London, Mem.*, 30, 135–143, 2004.
- 1330 Kosminska, K., Majka, J., Mazur, S., Krumbholz, M., Klonowska, I., Manecki, M., Czerny, J. and
 1331 Dwornik, M.: Blueschist facies metamorphism in Nordenskiöld Land of west-central
 1332 Svalbard, *Terra Nova*, 26, 377–386, 2014.
- 1333 Kostyuchenko, A., Sapozhnikov, R., Egorkin, A., Gee, D. G., Berzin, R. and Solodilov, L.: Crustal
 1334 structure and tectonic model of northeastern Baltica, based on deep seismic and potential
 1335 field data, in: *European Lithosphere Dynamics*, edited by: Gee, D. G. and Stephenson, R.
 1336 A., *Geol. Soc. London Mem.*, 32, 521–539, 2006.
- 1337 Labrousse, L., Elvevold, S., Lepvrier, C. and Agard, P.: Structural analysis of high-pressure
 1338 metamorphic rocks of Svalbard: Reconstructing the early stages of the Caledonian orogeny,
 1339 *Tectonics*, 27, 22 pp., 2008.
- 1340 Lamar, D. L. and Douglass, D. N.: Geology of an area astride the Billefjorden Fault Zone, Northern
 1341 Dicksonland, Spitsbergen, Svalbard, *Polarist. Skr.*, 197, 46 pp., 1995.
- 1342 Lamar, D. L., Reed, W. E. and Douglass, D. N.: Billefjorden fault zone, Spitsbergen: Is it part of a
 1343 major Late Devonian transform?, *GSA*, 97, 1083–1088, 1986.
- 1344 Larssen, G. B., Elvebakk, G., Henriksen, L. B., Kristensen, S.-E., Nilsson, I., Samuelsberg, T. J.,
 1345 Svånå, T. A., Stemmerik, L. and Worsley, D.: Upper Palaeozoic lithostratigraphy of the
 1346 Southern part of the Norwegian Barents Sea, *Norges geol. unders. Bull.*, 444, 45 pp., 2005.
- 1347 Lasabuda, A., Laberg, J. S., Knutsen, S.-M. and Safronova, P.: Cenozoic tectonostratigraphy and
 1348 pre-glacial erosion: A mass-balance study of the northwestern Barents Sea margin,
 1349 *Norwegian Arctic, J. Geodyn.*, 119, 149–166, 2018.
- 1350 Lippard, S. J. and Prestvik, T.: Carboniferous dolerite dykes on Magerøy: new age determination
 1351 and tectonic significance, *Norsk Geologisk Tidsskrift*, 77, 159–163, 1997.

- 1352 Livshits, Yu. Ya.: Tectonics of Central Vestspitsbergen, in: Geology of Spitsbergen, edited by:
1353 Sokolov, V. N., National Lending Library of Science and Technology, Boston Spa.,
1354 Yorkshire, UK, 59–75, 1965a.
- 1355 Livshits, Yu. Ya.: Paleogene deposits of Nordenskiöld Land, Vestspitsbergen, in: Geology of
1356 Spitsbergen, edited by: Sokolov, V. N., National Lending Library of Science and
1357 Technology, Boston Spa., Yorkshire, UK, 193–215, 1965b.
- 1358 Lopatin, B. G., Pavlov, L. G., Orgo, V. V. and Shkarubo, S. I.: Tectonic Structure of Novaya
1359 Zemlya, *Polarforschung*, 69, 131–135, 2001.
- 1360 Lorenz, H., Männik, P., Gee, D. and Proskurnin, V.: Geology of the Severnaya Zemlya Archipelao
1361 and the North Kara Terrane in the Russian high Arctic, *Int. J. Earth Sci.*, 97, 519–547, 2008.
- 1362 Lowell, J. D.: Spitsbergen tertiary Orogenic Belt and the Spitsbergen Fracture Zone, *GSA Bull.*,
1363 83, 3091–3102, 1972.
- 1364 Lyberis, N. and Manby, G.: Continental collision and lateral escape deformation in the lower and
1365 upper crust: An example from Caledonide Svalbard, *Tectonics*, 18, 1, 40–63, 1999.
- 1366 Majka, J. and Kosminska, K.: Magmatic and metamorphic events recorded within the Southwestern
1367 Basement Province of Svalbard, *Arktos*, 3:5, 2017.
- 1368 Majka, J., Mazur, S., Manecki, M., Czerny, J. and Holm, D. K.: Late Neoproterozoic amphibolite-
1369 facies metamorphism of a pre-Caledonian basement block in southwest Wedel Jarlsberg
1370 Land, Spitsbergen: new evidence from U–Th–Pb dating of monazite, *Geol. Mag.*, 145, 6,
1371 822–830, 2008.
- 1372 Majka, J., Larionov, A. N., Gee, D. G., Czerny, J. and Prsek, J.: Neoproterozoic pegmatite from
1373 Skoddefjellet, Wedel Jarlsberg Land, Spitsbergen: Additional evidence for c. 640 Ma
1374 tectonothermal event in the Caledonides of Svalbard, *Polish Polar Res.*, 33, 1–17, 2012.
- 1375 Majka, J., De’eri-Shlevin, Y., Gee, D. G., Czerny, J., Frei, D. and Ladenberger, A.: Torellian (c.
1376 640 Ma) metamorphic overprint of Tonian (c. 950 Ma) basement in the Caledonides of
1377 southwestern Svalbard, *Geol. Mag.*, 151, 4, 732–748, 2014.
- 1378 Manby, G. M. and Lyberis, N.: Tectonic evolution of the Devonian Basin of northern Spitsbergen,
1379 *Norsk Geol. Tidsskr.*, 72, 7–19, 1992.
- 1380 Manby, G. M., Lyberis, N., Chorowicz, J. and Thiedig, F.: Post-Caledonian tectonics along the
1381 Billefjorden fault zone, Svalbard, and implications for the Arctic region, *Geol. Soc. Am.*
1382 *Bul.*, 105, 201–216, 1994.

- 1383 Manecki, M., Holm, D. K., Czerny, J. and Lux, D.: Thermochronological evidence for late
1384 Proterozoic (Vendian) cooling in southwest Wedel Jarlsberg Land, Spitsbergen, Geological
1385 Magazine, 135, 63–9, 1998.
- 1386 Mareello, L., Ebbing, J. and Gernigon, L.: Magnetic basement study in the Barents Sea from
1387 inversion and forward modelling, Tectonophys., 493, 153–171, 2010.
- 1388 Mareello, L., Ebbing, J. and Gernigon, L.: Basement inhomogeneities and crustal setting in the
1389 Barents Sea from a combined 3D gravity and magnetic model, Geophys. J. Int., 193, 2,
1390 557–584, 2013.
- 1391 Mazur, S., Czerny, J., Majka, J., Manecki, M., Holm, D., Smyrak, A. and Wypych, A.: A strike-
1392 slip terrane boundary in Wedel Jarlsberg Land, Svalbard, and its bearing on correlations of
1393 SW Spitsbergen with the Pearya terrane and Timanide belt, J. Geol. Soc. London, 166, 529–
1394 544, 2009.
- 1395 McCann, A. J.: Deformation of the Old Red Sandstone of NW Spitsbergen; links to the Ellesmerian
1396 and Caledonian orogenies, in: New Perspectives on the Old Red Sandstone, edited by:
1397 Friends, P. F. and Williams, B. P. J., Geol. Soc. London, 180, 567–584, 2000.
- 1398 Merdith, A. S., Williams, S. E., Collins, A. S., Tetley, M. G., Mulder, J. A., Blades, M. L., Young,
1399 A., Armistead, S. E., Cannon, J., Zahirovic, S. and Müller, R. D.: Extending full-plate
1400 tectonic models into deep time: Linking the Neoproterozoic and the Phanerozoic, Earth-
1401 Sci. Rev., 214, 103477, 2021.
- 1402 Müller, R., Klausen, T. G., Faleide, J. I., Olaussen, S., Eide, C. H. and Suslova, A.: Linking regional
1403 unconformities in the Barents Sea to compression-induced forebulge uplift at the Triassic-
1404 Jurassic transition, Tectonophys., 765, 35–51, 2019.
- 1405 Murascov, L. G. and Mokin, Ju. I.: Stratigraphic subdivision of the Devonian deposits of
1406 Spitsbergen, Polarinst. Skr., 167, 249–261, 1979.
- 1407 Nasuti, A., Roberts, D. and Gernigon, L.: Multiphase mafic dykes in the Caledonides of northern
1408 Finnmark revealed by a new high-resolution aeromagnetic dataset, Norwegian Journal of
1409 Geology, 95, 251–263, 2015.
- 1410 Norton, M. G., McClay, K. R. and Way, N. A.: Tectonic evolution of Devonian basins in northern
1411 Scotland and southern Norway, Norsk Geol. Tidsskr., 67, 323–338, 1987.

1412 Oakey, G. N. and Chalmers, J. A.: A new model for the Paleogene motion of Greenland relative to
 1413 North America: Plate reconstructions of the Davis Strait and Nares Strait regions between
 1414 Canada and Greenland, *J. of Geophys. Res.*, 117, B10401, 2012.

1415 Ogata, K., Mulrooney, M. J., Braathen, A., Maher, H., Osmundsen, P. T., Anell, I., Smyrak-Sikora,
 1416 A. A. and Balsamo, F.: Architecture, deformation style and petrophysical properties of
 1417 growth fault systems: the Late Triassic deltaic succession of southern Edgeøya (East
 1418 Svalbard), *Basin Res.*, 30, 5, 1042–1073, 2018.

1419 Ohta, Y., Dallmeyer, R. D. and Peucat, J. J.: Caledonian terranes in Svalbard, *GSA Spec. Paper*,
 1420 230, 1–15, 1989.

1421 Ohta, Y., Krasil'scikov, A. A., Lepvrier, C. and Teben'kov, A. M.: Northern continuation of
 1422 Caledonian high-pressure metamorphic rocks in central-western Spitsbergen, *Polar Res.*,
 1423 14, 3, 303–315, 1995.

1424 Olovyanishshnikov, V. G., Roberts, D. and Siedlecka, A.: Tectonics and Sedimentation of the
 1425 Meso- to Neoproterozoic Timan-Varanger Belt along the Northeastern Margin of Baltica,
 1426 *Polarforschung*, 68, 267–274, 2000.

1427 Osmundsen, P-T., Braathen, A., Rød, R. S. and Hynne, I. B.: Styles of normal faulting and fault-
 1428 controlled sedimentation in the Triassic deposits of Eastern Svalbard, *Norwegian Petroleum*
 1429 *directorates Bulletin*, 10, 61–79, 2014.

1430 Petersen, T. G., Thomsen, T. B., Olaussen, S. and Stemmerik, L.: Provenance shifts in an evolving
 1431 Eurekan foreland basin: the Tertiary Central Basin, Spitsbergen, *J. Geol. Soc., London*, 173,
 1432 634–648, 2016.

1433 Peucat, J.-J., Ohta, Y., Gee, D. G. and Bernard-Griffiths, J.: U-Pb, Sr and Nd evidence for
 1434 Grenvillian and latest Proterozoic tectonothermal activity in the Spitsbergen Caledonides,
 1435 *Arctic Ocean, Lithos*, 22, 275–285, 1989.

1436 Phillips, T., Jackson, C. A-L., Bell, R. E., Duffy, O. B. and Fossen, H.: Reactivation of
 1437 intrabasement structures during rifting: A case study from offshore southern Norway,
 1438 *Journal of Structural Geology*, 91, 54–73, 2016.

1439 Piepjohn, K.: The Svalbardian–Ellesmerian deformation of the Old Red Sandstone and the pre-
 1440 Devonian basement in NW Spitsbergen (Svalbard), in: *New Perspectives on the Old Red*
 1441 *Sandstone*, edited by: Friend, P. F. and Williams, B. P. J., *Geol. Soc. London Spec. Publi.*,
 1442 180, 585–601, 2000.

- 1443 Piepjohn, K.: von Gosen, W., Läuffer, A., McClelland, W. C. and Estrada, S.: Ellesmerian and
 1444 Eureka fault tectonics at the northern margin of Ellesmere Island (Canadian High Arctic),
 1445 Z. Dt. Ges. Geowiss., 164, 1, 81–105, 2013.
- 1446 Piepjohn, K., Dallmann, W. K. and Elvevold, S.: The Lomfjorden Fault Zone in eastern Spitsbergen
 1447 (Svalbard), in: Circum-Arctic Structural Events: Tectonic Evolution of the Arctic Margins
 1448 and Trans-Arctic Links with Adjacent Orogens, edited by: Piepjohn, K., Strauss, J. V.,
 1449 Reinhardt, L. and McClelland, W. C., GSA Spec. Paper, 541, 95–130, 2019.
- 1450 Ramsay, J. G.: Interference Patterns Produced by the Superposition of Folds of Similar Type, J.
 1451 Geol., 70, 4, 466–481, 1962.
- 1452 Rice, A. H. N.: Restoration of the External Caledonides, Finnmark, North Norway, in: New
 1453 Perspectives on the Caledonides of Scandinavia and Related Areas, Corfu, F., Gasser, D.
 1454 and Chew, D. M. (eds), Geological Society, London, Special Publications, 390, 271–299,
 1455 2014.
- 1456 Roberts, D.: Tectonic Deformation in the Barents Sea Region of Varanger Peninsula, Finnmark,
 1457 Norges geol. unders., 282, 1–39, 1972.
- 1458 Roberts, D. and Olovyanishnikov, V.: Structural and tectonic development of the Timanide
 1459 orogeny, in: The Neoproterozoic Timanide Orogen of Eastern Baltica, edited by: Gee, D.
 1460 G. and Pease, V., Geol. Soc. London, Mem., 30, 47–57, 2004.
- 1461 Roberts, D. and Siedlecka, A.: Timanian orogenic deformation along the northeastern margin of
 1462 Baltica, Northwest Russia and Northeast Norway, and Avalonian-Cadomian connections,
 1463 Tectonophysics, 352, 169–184, 2002.
- 1464 Roberts, D. and Williams, G. D.: Berggrunnskart Kjøllefjord 2236 IV, M 1:50.000, foreløpig
 1465 utgave, Norges geol. unders., 2013.
- 1466 Roberts, D., Mitchell, J. G. and Andersen, T. B.: A post-Caledonian dyke from Magerøy North
 1467 Norway: age and geochemistry, Norwegian Journal of Geology, 71, 289–294, 1991.
- 1468 Rosa, D., Majka, J., Thrane, K. and Guarnieri, P.: Evidence for Timanian-age basement rocks in
 1469 North Greenland as documented through U–Pb zircon dating of igneous xenoliths from the
 1470 Midtkap volcanic centers, Precambrian Res., 275, 394–405, 2016.
- 1471 Schiffer, C., Doré, A. G., Foulger, G. R., Franke, D., Geoffroy, L., Gernigon, L., Holdsworth, B.,
 1472 Kuszniir, N., Lundin, E., McCaffrey, K., Peace, A. L., Petersen, K. D., Phillips, T. B.,

1473 Stephenson, R., Stoker, M. S. and Welford, J. K.: Structural inheritance in the North
1474 Atlantic, *Earth-Science Reviews*, 206, 102975, 2020.

1475 Senger, K., Roy, S., Braathen, A., Buckley, S., Bælum, K., Gernigon, L., Mjelde, R., Noormets,
1476 R., Ogata, K., Olaussen, S., Planke, S., Ruud, B. O. and Tveranger, J.: Geometries of
1477 doleritic intrusions in central Spitsbergen, Svalbard: an integrated study of an onshore-
1478 offshore magmatic province with applications to CO₂ sequestration, *Norw. J. Geol.*, 93,
1479 143–166, 2013.

1480 Siedlecka, A.: Late Precambrian Stratigraphy and Structure of the North-Eastern Margin of the
1481 Fennoscandian Shield (East Finnmark – Timan Region), *Nor. geol. unders.*, 316, 313-348,
1482 1975.

1483 Siedlecka, A. and Roberts, D.: Report from a visit to the Komi Branch of the Russian Academy of
1484 Sciences in Syktyvkar, Russia, and from fieldwork in the central Timans, August 1995,
1485 Norges geol. unders. report, 95.149, 32 pp., 1995.

1486 Siedlecka, A. and Siedlecki, S.: Some new aspects of the geology of Varanger peninsula (Northern
1487 Norway), *Nor. geol. unders.*, 247, 288-306, 1967.

1488 Siedlecka, A. and Siedlecki, S.: Late Precambrian sedimentary rocks of the Tanafjord–
1489 Varangerfjord region of Varanger Peninsula, Northern Norway, in: *The Caledonian*
1490 *Geology of Northern Norway*, edited by: Roberts, D. and Gustavson, M., *Norges geol.*
1491 *unders.*, 269, 246–294, 1971.

1492 Smyrak-Sikora, A., Osmundsen, P. T., Braathen, A., Ogata, K., Anell, I., Mulrooney, M. J. and
1493 Zuchuat, V: Architecture of growth basins in a tidally influenced, prodelta to delta-front
1494 setting: The Triassic succession of Kvalpynten, East Svalbard, *Basin Research*, 32, 5, 959–
1495 988, 2020.

1496 Stouge, S., Christiansen, J. L. and Holmer, L. E.: Lower Palaeozoic stratigraphy of
1497 Murchisonfjorden and Sparreneset, Nordaustlandet, Svalbard, *Geografiska Annaler: Series*
1498 A, *Physical Geography*, 93, 209–226, 2011.

1499 Sturt, B. A., Pringle, I. R. and Ramsay, D. M.: The Finnmarkian phase of the Caledonian Orogeny,
1500 *J. Geol., Soc., London*, 135, 597–610, 1978.

1501 Thiede, J., Pfirman, S., Schenke, H.-W. and Reil, W.: Bathymetry of Molloy Deep: Fram Strait
1502 Between Svalbard and Greenland, *Mar. Geophys. Res.*, 12, 197–214, 1990.

1503 Tonstad, S. A.: The Late Paleozoic development of the Ottar basin from seismic 3D interpretation,
 1504 Master's Thesis, University of Tromsø, Tromsø, Norway, 135 pp., 2018.

1505 Torsvik, T. H. and Trench, A.: The Ordovician history of the Iapetus Ocean in Britain: new
 1506 palaeomagnetic constraints, *J. Geol. Soc.*, London, 148, 423–425, 1991.

1507 Torsvik, T. H., Burke, K., Steinberger, B., Webb, S. J. and Ashwal, L. D.: Diamond sampled by
 1508 plumes from the core–mantle boundary, *Nature Lett.*, 466, 352–355, 2010.

1509 Townsend, C.: Thrust transport directions and thrust sheet restoration in the Caledonides of
 1510 Finnmark, North Norway, *J. Structural Geol.*, 9, 3, 345–352, 1987.

1511 Vernikovsky, V. A., Metelkin, D. V., Vernikovskaya, A. E., Matushkin, N. Yu., Lobkovsky, L. I.
 1512 and Shipilov, E. V.: Early evolution stage of the arctic margins (Neoproterozoic-Paleozoic)
 1513 and plate reconstructions, *ICAM VI Proceedings*, May 2011, Fairbanks, Alaska, USA, 265–
 1514 285, 2011.

1515 Von Gosen, W. and Piepjohn, K.: Polyphase Deformation in the Eastern Hornsund Area, *Geol. Jb.*,
 1516 B91, 291–312, 2001.

1517 Witt-Nilsson, P., Gee, D. G. and Hellman, F. J.: Tectonostratigraphy of the Caledonian Atomfjella
 1518 Antiform of northern Ny Friesland, Svalbard, *Norsk Geol. Tidsskr.*, 78, 67–80, 1998.

1519 Worsley, D., Agdestein, T., Gjelberg, J. G., Kirkemo, K., Mørk, A., Nilsson, I., Olaussen, S., Steel,
 1520 R. J. and Stemmerik, L.: The geological evolution of Bjørnøya, Arctic Norway:
 1521 implications for the Barents Shelf, *Norsk Geol. Tidsskr.*, 81, 195–234, 2001.

1522 Ziegler, P. A.: Evolution of the Arctic–North Atlantic and the Western Tethys, *AAPG Mem.* 43,
 1523 1988.

1524

1525 **Figures**

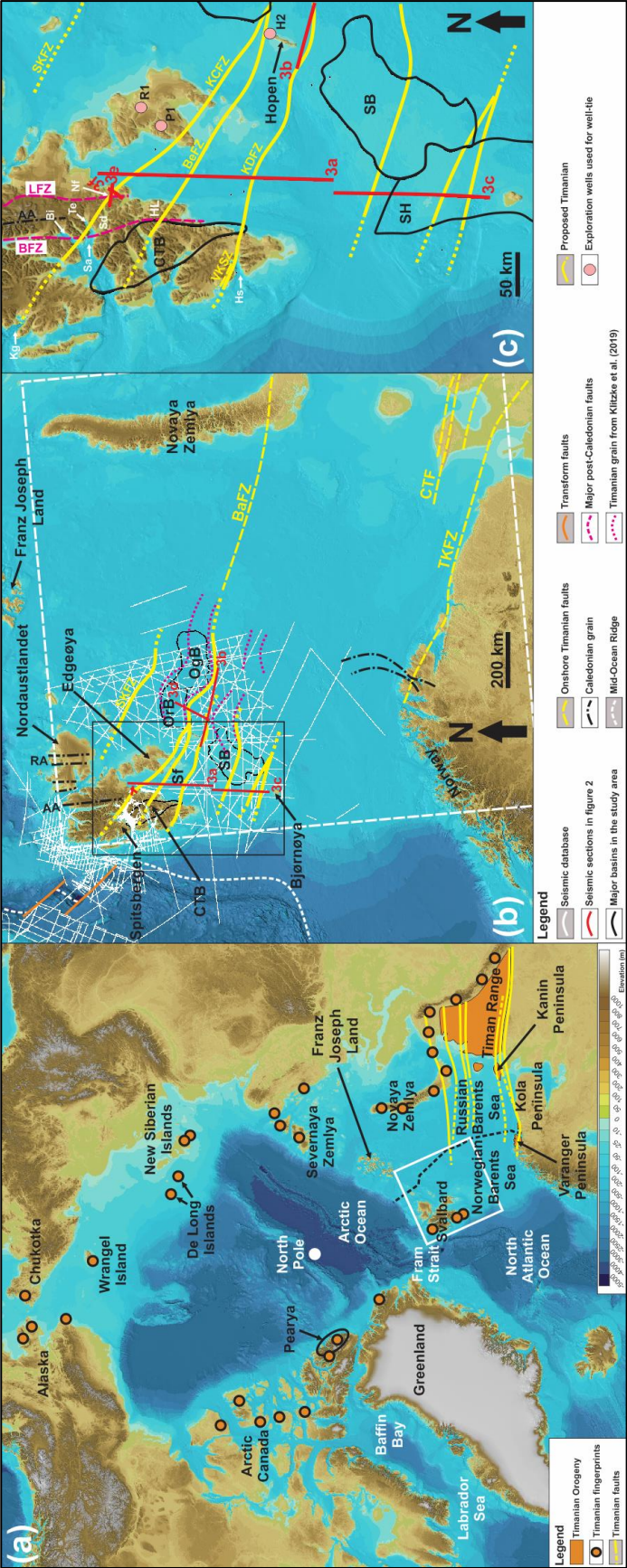


Figure 1: (a) Overview map showing the Timanian belt in Russia and Norway, and occurrences of Timanian fingerprints throughout the Arctic; (b) Regional map of Svalbard and the Barents Sea the main geological elements and the seismic database used in the present study. The location of (b) is shown as a white frame in (a); (c) Zoom in the northern Norwegian Barents Sea and Svalbard showing the main faults and basins in the study area, and the proposed Timanian structures. The location of (c) is shown as a black frame in (b). The location of the Raddedalen-1 well is from Smyrak-Sikora et al. (2020). Topography and bathymetry are from Jakobsson et al. (2012). Abbreviations: AA: Atomfjella Antiform; BaFZ: Baidaratsky fault zone; BeFZ: Bellsundbanken fault zone; BFZ: Billefjorden Fault Zone; Bi: Billefjorden; CTB: Central Tertiary Basin; HL: Heer Land; Hs: Hornsund; H2: Hopen-2; KCFZ: Kongsfjorden–Cowanodden fault zone; KDFZ: Kinnhøgda–Daudbjørnpynten fault zone; Kg: Kongsfjorden; LFZ: Lomfjorden Fault Zone; Nf: Nordmannsfonna; OgB: Olga Basin; OrB: Ora Basin; P1: Plurdalen-1; RA: Rijpdalen Anticline; R1: Raddedalen-1; Sa: Sassenfjorden; SB: Sørkapp Basin; Sf: Storfjorden; SH: Stappen High; SKFZ: Steiløya–Krylen fault zone; Te: Tempelfjorden; TKFZ: Trollfjorden–Komagelva Fault Zone; VKSZ: Vimsodden–Kosibapasset Shear Zone.

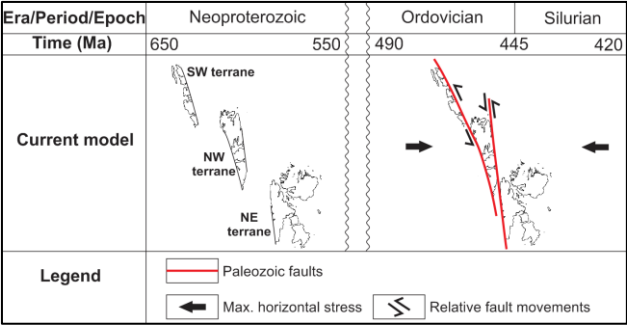
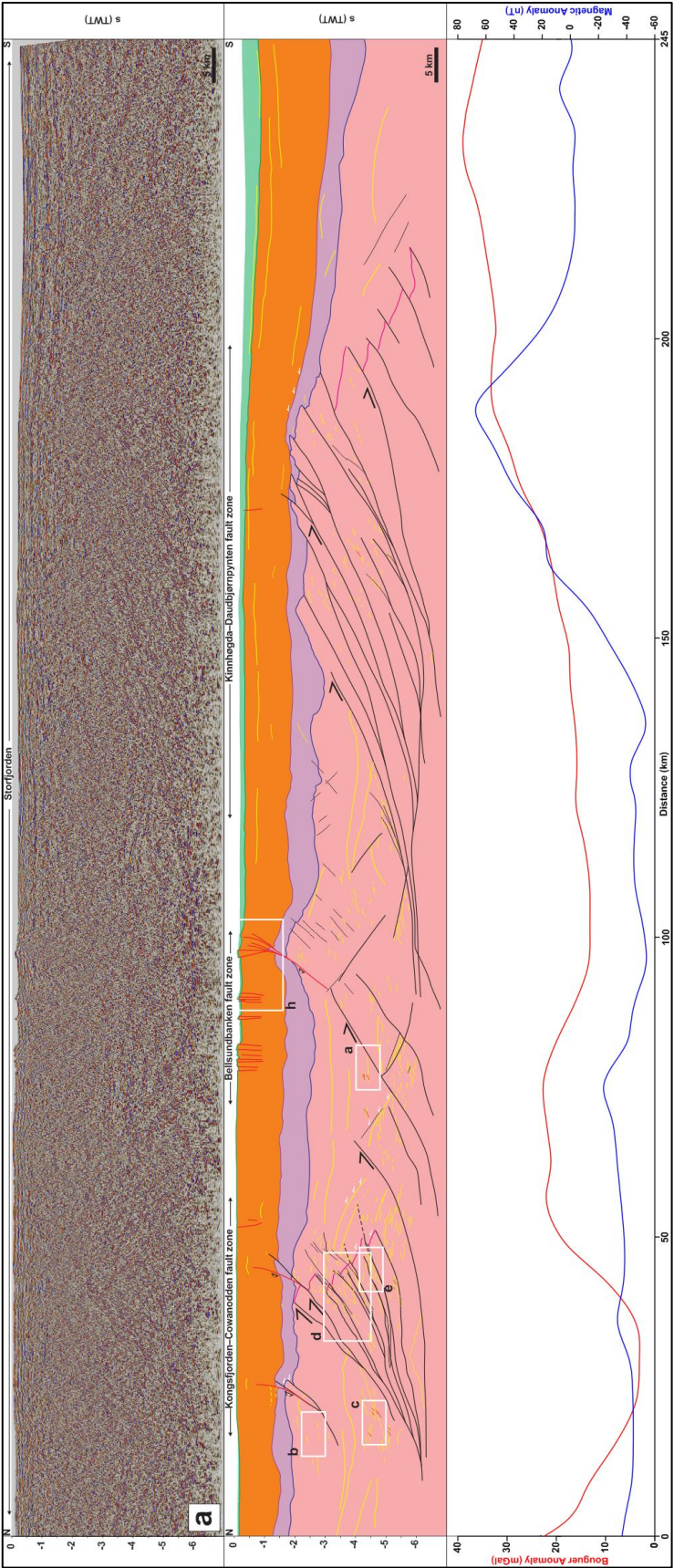
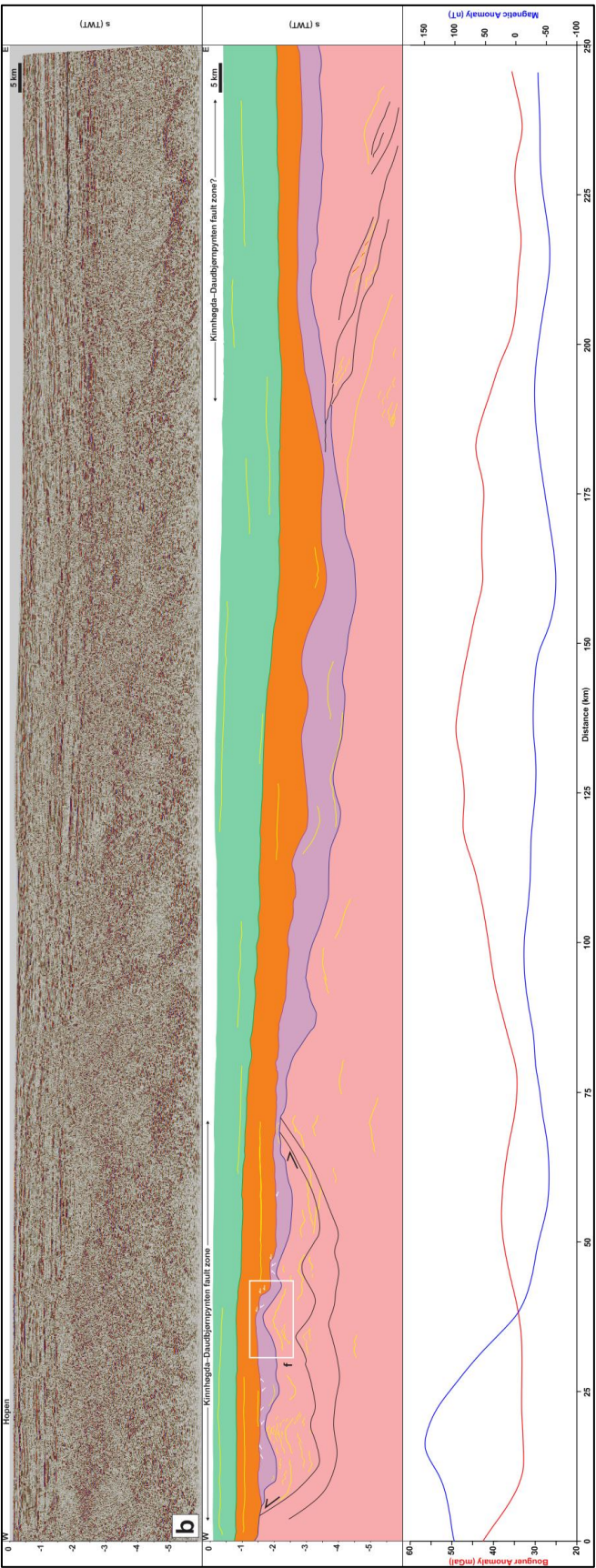
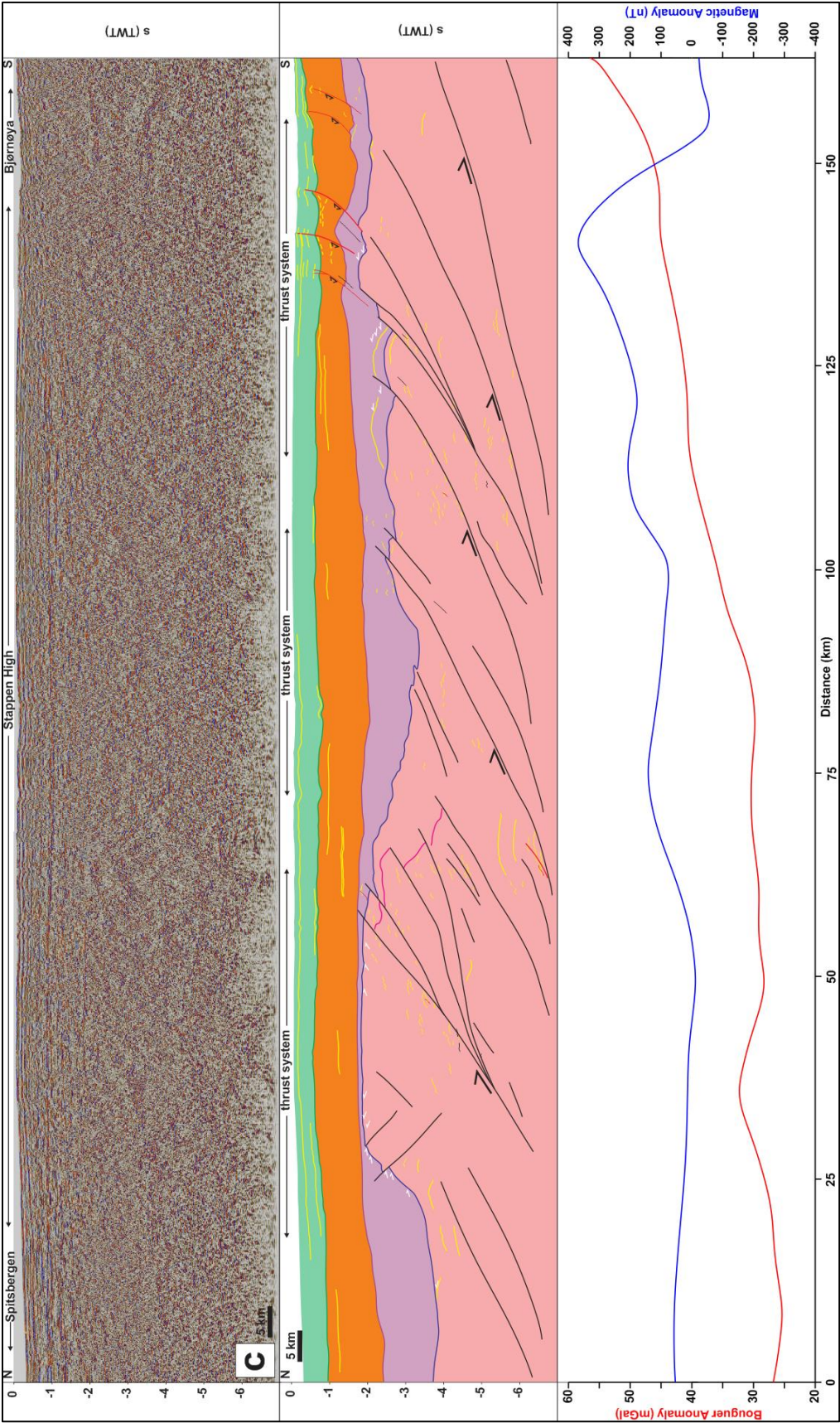
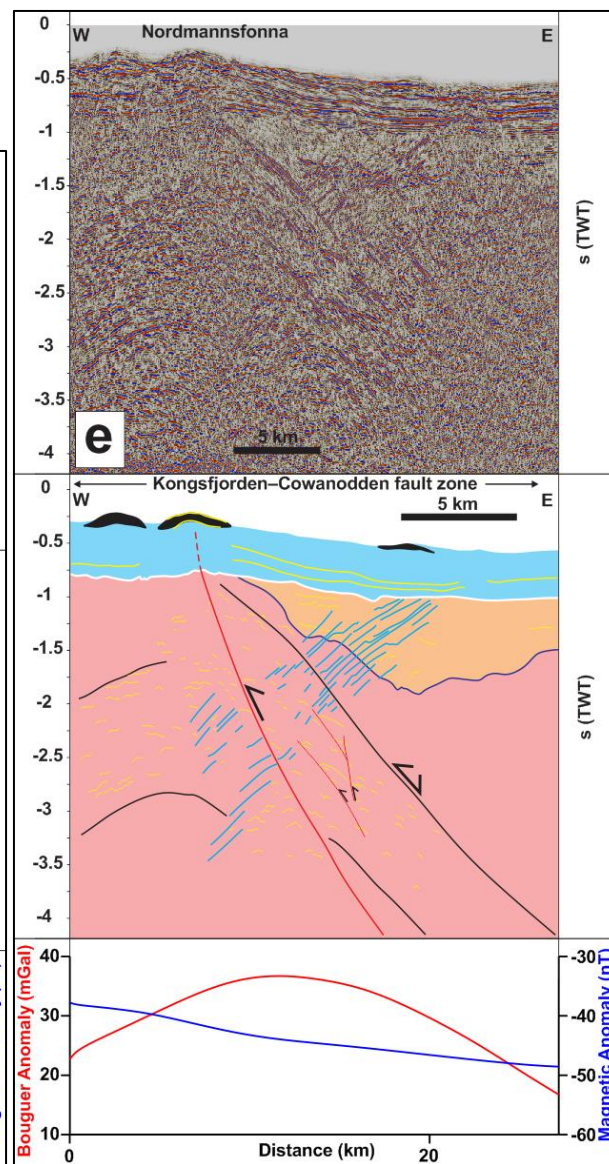
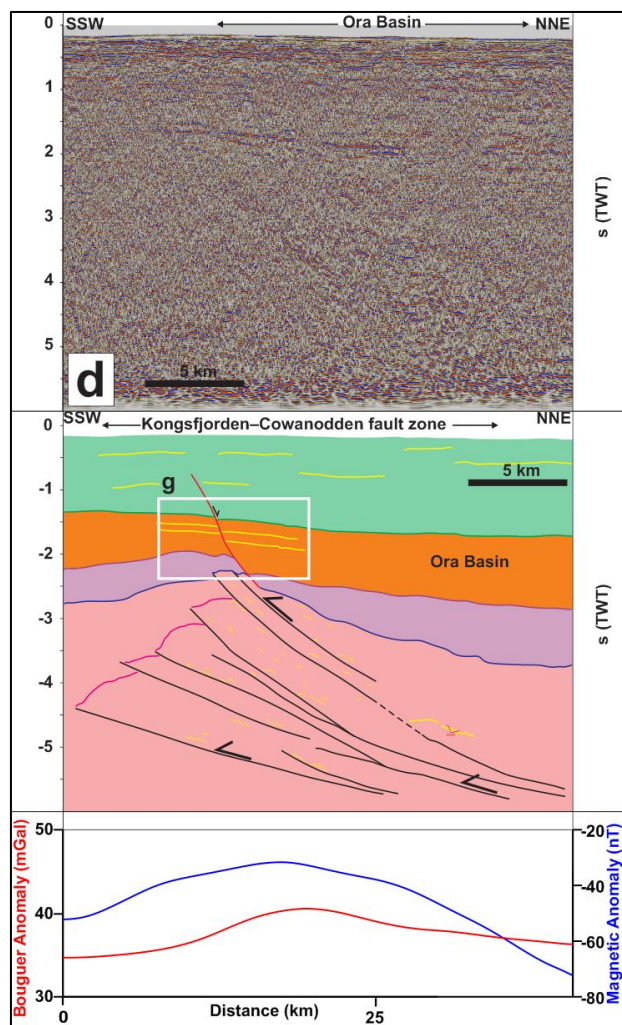


Figure 2: Paleogeographic reconstruction of the Svalbard Archipelago in the latest Neoproterozoic during the Timanian Orogeny and in the early–mid Paleozoic during the Caledonian Orogeny according to previous models (e.g., Harland, 1969; Labrousse et al., 2008).









1546

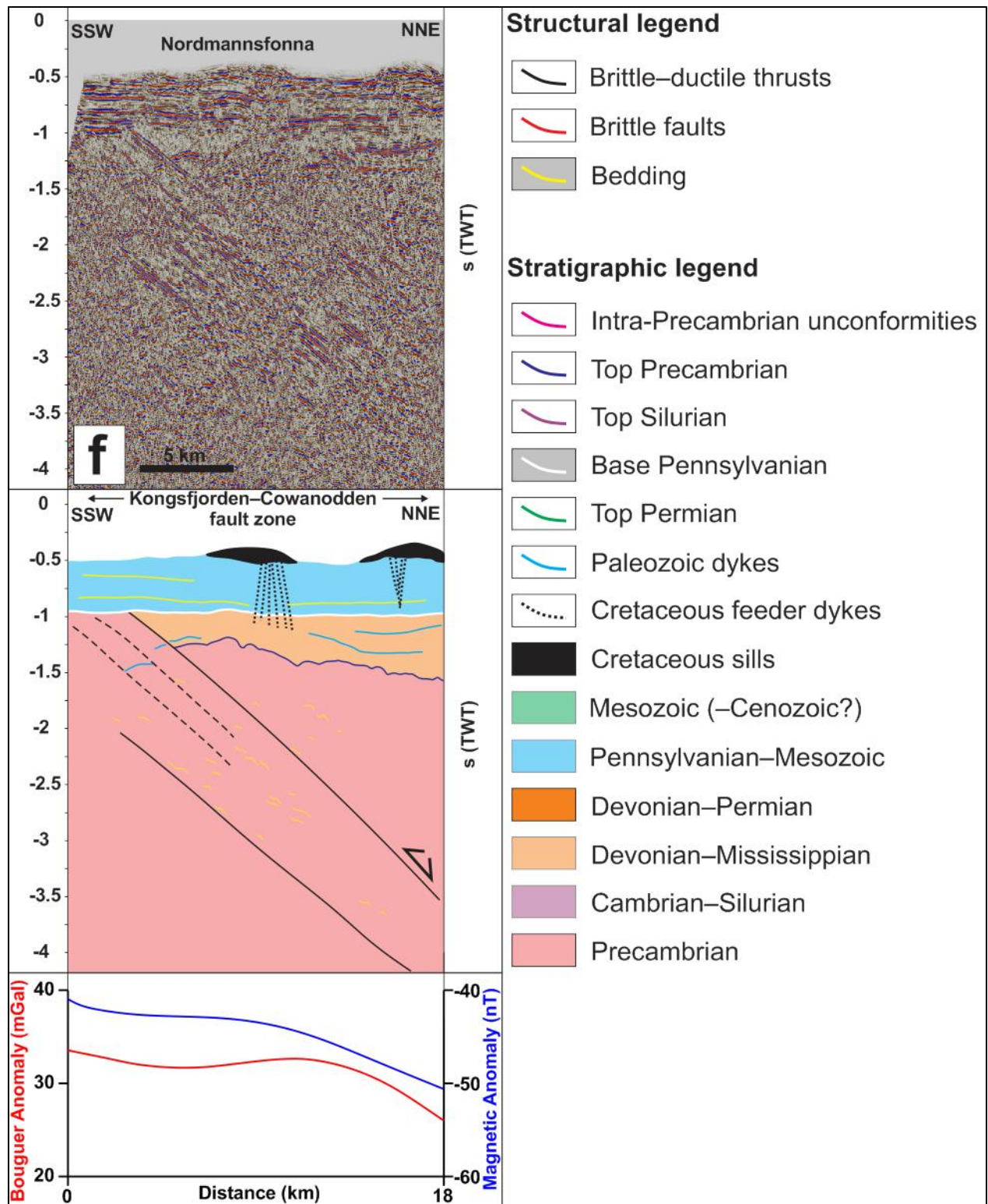


Figure 3: Interpreted seismic profiles and associated potential field data (a) in Storfjorden, (b) south of Hopen, (c) on the Stappen High in the northwestern Norwegian Barents Sea between Spitsbergen and Bjørnøya, (d) on the southern flank of the Ora Basin in the northeastern Norwegian Barents Sea, and (e and f) in Nordmannsfonna in eastern Spitsbergen. The seismic profiles show top-SSW Timanian thrusts that were reactivated and overprinted during subsequent tectonic events such as Caledonian contraction, Devonian-Carboniferous late-post Caledonian collapse and rifting, Eurekan contraction, and present-day contraction. Profiles (e) and (f) also show Paleozoic and Cretaceous intrusions. The white frames show the

1554 location of zoomed-in portions of the profiles displayed in Figure 4. Potential field data below the seismic profiles include
1555 Bouguer anomaly (red lines) and magnetic anomaly (blue lines). The potential field data show consistently high gravimetric
1556 anomalies and partial correlation with high magnetism towards the footwall of each major thrust systems (i.e., towards
1557 thickened portions of the crust).

1558

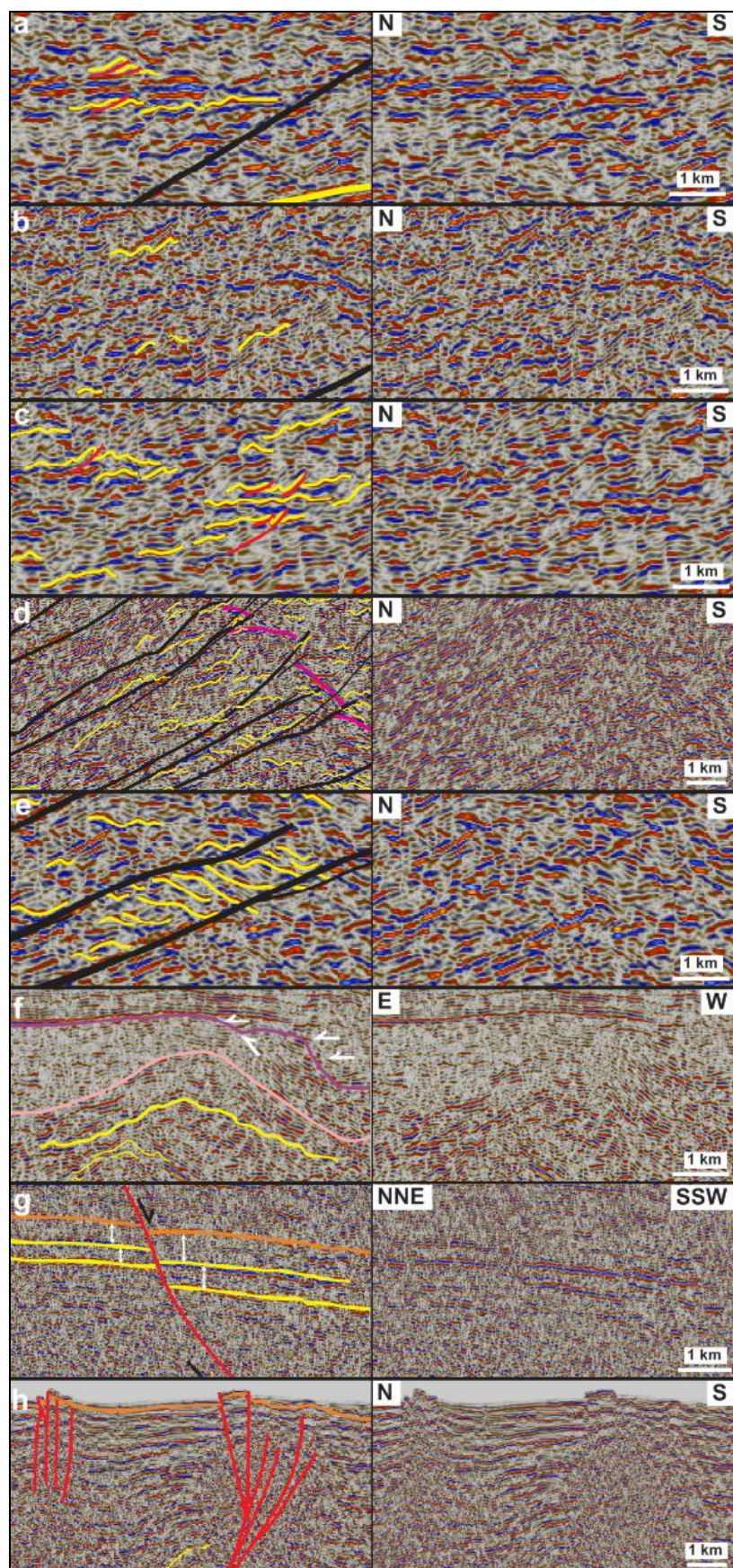


Figure 4: Zooms in seismic profiles shown in Figure 3 showing (a) upright fold structures, (b) SSW-verging folds and (c) top-SSW minor thrusts in Precambrian–lower Paleozoic (meta-) sedimentary basement rocks, (d) SSW-verging folds and NNE-dipping mylonitic shear zones within a major thrust that offsets major basement unconformities (fuchsia lines) top-SSW, (e) duplex structures within a major top-SSW thrust, (f) a N–S- to NNE–SSW-trending, 5–15 kilometers wide, symmetrical, upright macro-fold and associated, kilometer- to hundreds of meter-scale, parasitic macro- to meso-folds, (g) syn-tectonic thickening in Devonian–Carboniferous (–Permian?) sedimentary strata offset down-NNE by a normal fault that merges with a thick mylonitic shear zone at depth, and (h) recent–ongoing reverse offsets of the seafloor reflection by multiple, inverted, NNE-dipping normal faults in Storfjorden. See Figure 3 for location of each zoom and for legend.

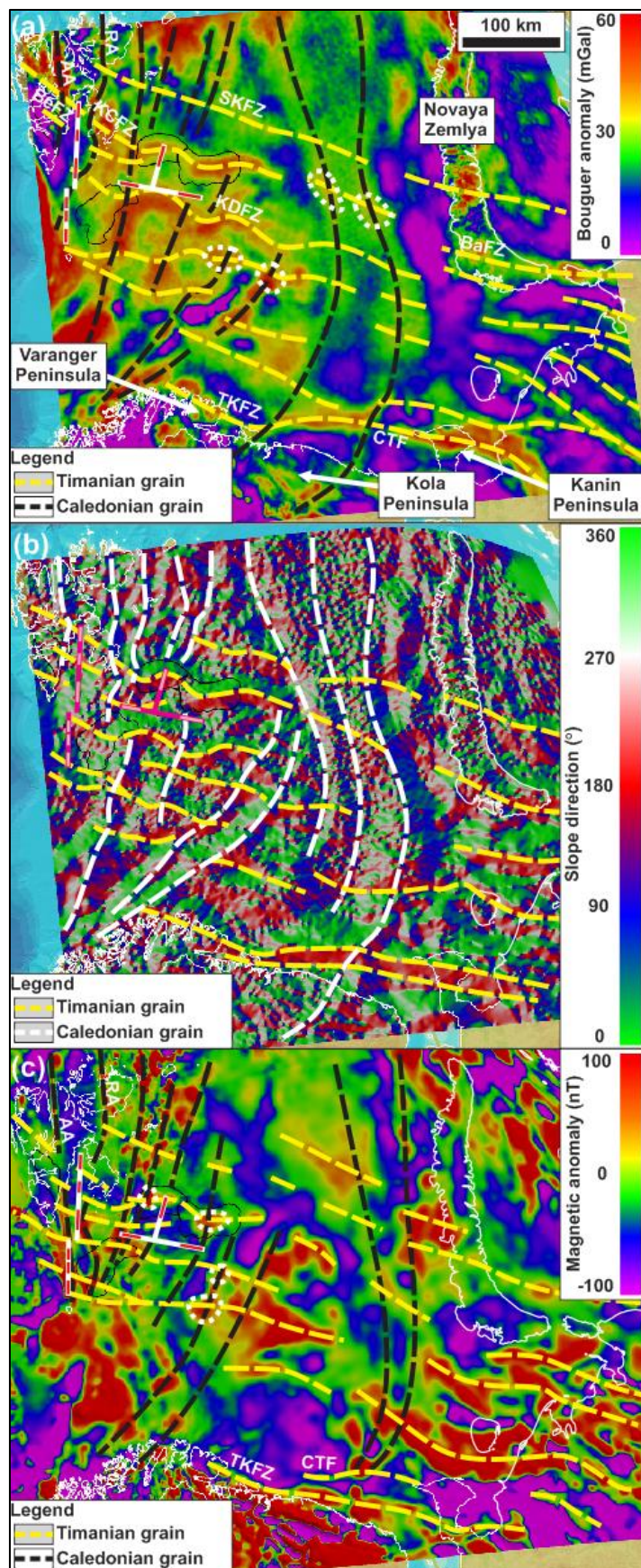


Figure 5: Gravimetric (a and b) and magnetic (c) anomaly maps over the Barents Sea and adjacent onshore areas in Russia (see location as a dashed white frame in Figure 1b), Norway and Svalbard showing E–W- to NW–SE-trending anomalies (dashed yellow lines) that correlate with the proposed NNE-dipping Timanian thrust systems in Svalbard and the northern Norwegian Barents Sea. Note the high obliquity of E–W- to NW–SE-trending Timanian grain with NE–SW- to N–S-trending Caledonian grain (dashed black/white lines). Note that dashed lines in (a) and (c) denote high gravimetric and magnetic anomalies. Also notice the oval-shaped high gravimetric and magnetic anomalies (dotted white lines) at the intersection of WNW–ESE- and N–S- to NNE–SSW-trending anomalies in (a) and (c) resulting from the interaction of the two (Timanian and Caledonian) thrust and fold trends. The location of seismic profiles presented in Figure 3a–d are shown as thick white lines in (a) and (c) and as fuchsia lines in (b). Within these thick white and fuchsia lines, the location and extent of thrust systems evidenced on seismic data (Figure 3) is shown in white in (a) and (c) and in pink in (b). For the E–W-trending seismic profile shown in Figure 3b, this implies that the red and pink lines represent N–S-trending synclines. Abbreviations: AA: Atomfjella Antiform; BaFZ: Baidaratsky fault zone; BeFZ: Bellsundbanken fault zone; CTF: Central Timan Fault; KCFZ: Kongsfjorden–Cowanodden fault zone; KDFZ: Kinnhøgda–Daudbjørnpynnten fault zone; RA: Rijpdalen Anticline; SKFZ: Steiløya–Krylen fault zone; TKFZ: Trollfjorden–Komagelva Fault Zone.

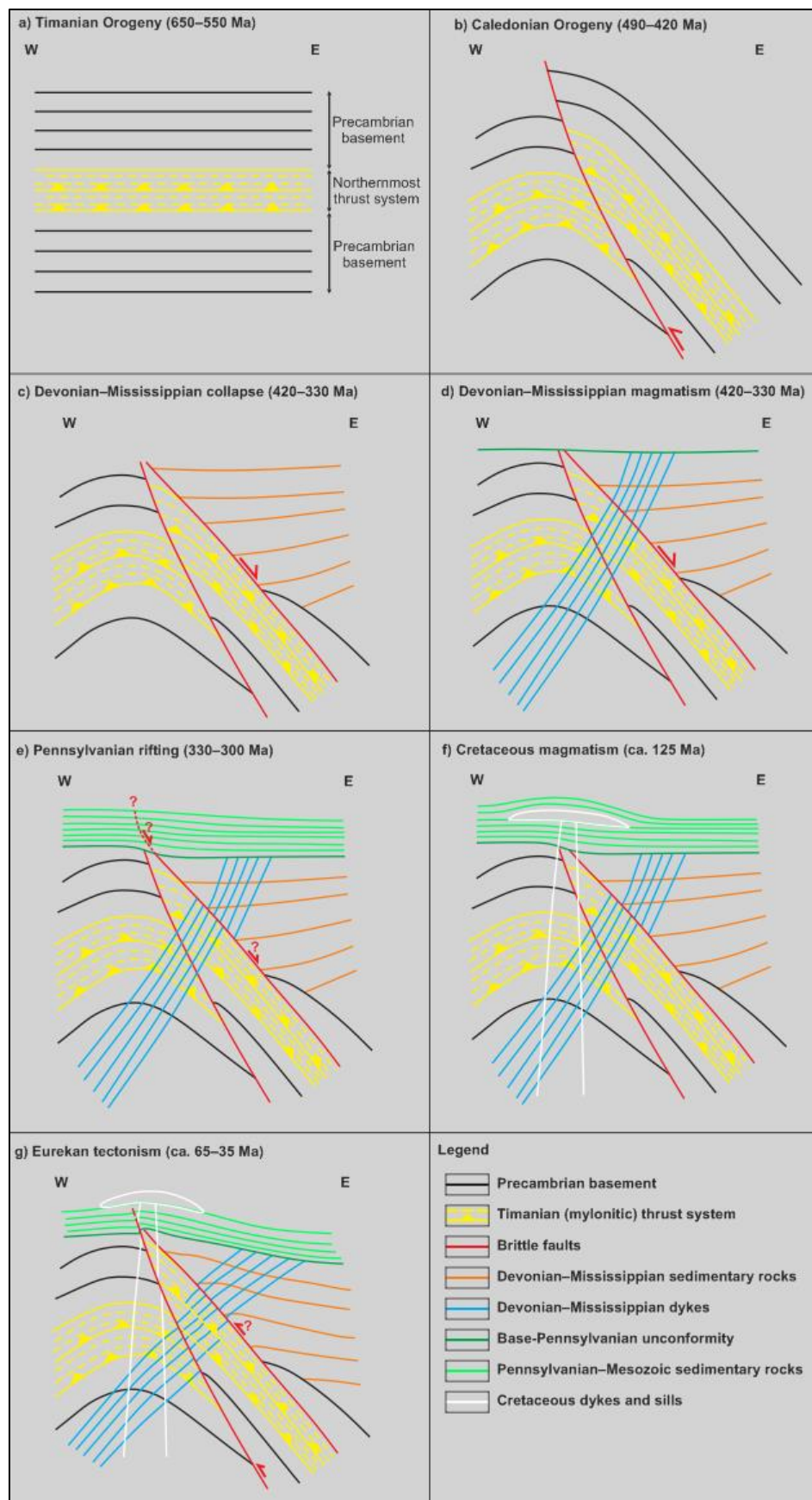


Figure 6: Sketches showing a possible reconstruction of the tectonic history of the E–W seismic profile in Nordmannsfonna shown in Figure 3e. (a) Formation of a NNE-dipping, mylonitic thrust system (Kongsfjorden–Cowanodden fault zone) within Precambrian basement rocks during the Timanian Orogeny in the latest Neoproterozoic. The NNE-dipping Kongsfjorden–Cowanodden fault zone appears near horizontal on the E–W transect; (b) Top-west thrusting along the east-dipping Agardhbukta Fault and folding of the Kongsfjorden–Cowanodden fault zone into a broad, moderately NNE-plunging anticline during the Caledonian Orogeny; (c) Inversion of the Kongsfjorden–Cowanodden fault zone along the eastern flank of the Caledonian anticline and deposition of thickened, gently west-dipping, syn-tectonic, Devonian (–Mississippian?) sedimentary strata during post-Caledonian collapse-related extension; (d) Intrusion of Precambrian basement and Devonian (–Mississippian?) sedimentary rocks by steeply west-dipping dykes in the Devonian–Mississippian; (e) Regional erosion in the mid-Carboniferous (latest Mississippian) and deposition of Pennsylvanian sedimentary strata, possibly along a high-angle brittle splay of the inverted portion of the Kongsfjorden–Cowanodden fault zone during rift-related extension; (f) Deposition of Mesozoic sedimentary strata and intrusion of Cretaceous dolerite dykes and sills; (g) Erosion of Pennsylvanian–Mesozoic strata and reactivation of the Kongsfjorden–Cowanodden fault zone and Agardhbukta Fault with minor reverse movements in the early Cenozoic during the Eurekan tectonic event as shown by mild folding and offset of overlying post-Caledonian sedimentary strata, dykes and Base-Pennsylvanian unconformity. Also note the back-tilting (i.e., clockwise rotation) of Devonian–Mississippian dykes in the hanging wall of the Agardhbukta Fault and of the Kongsfjorden–Cowanodden fault zone.

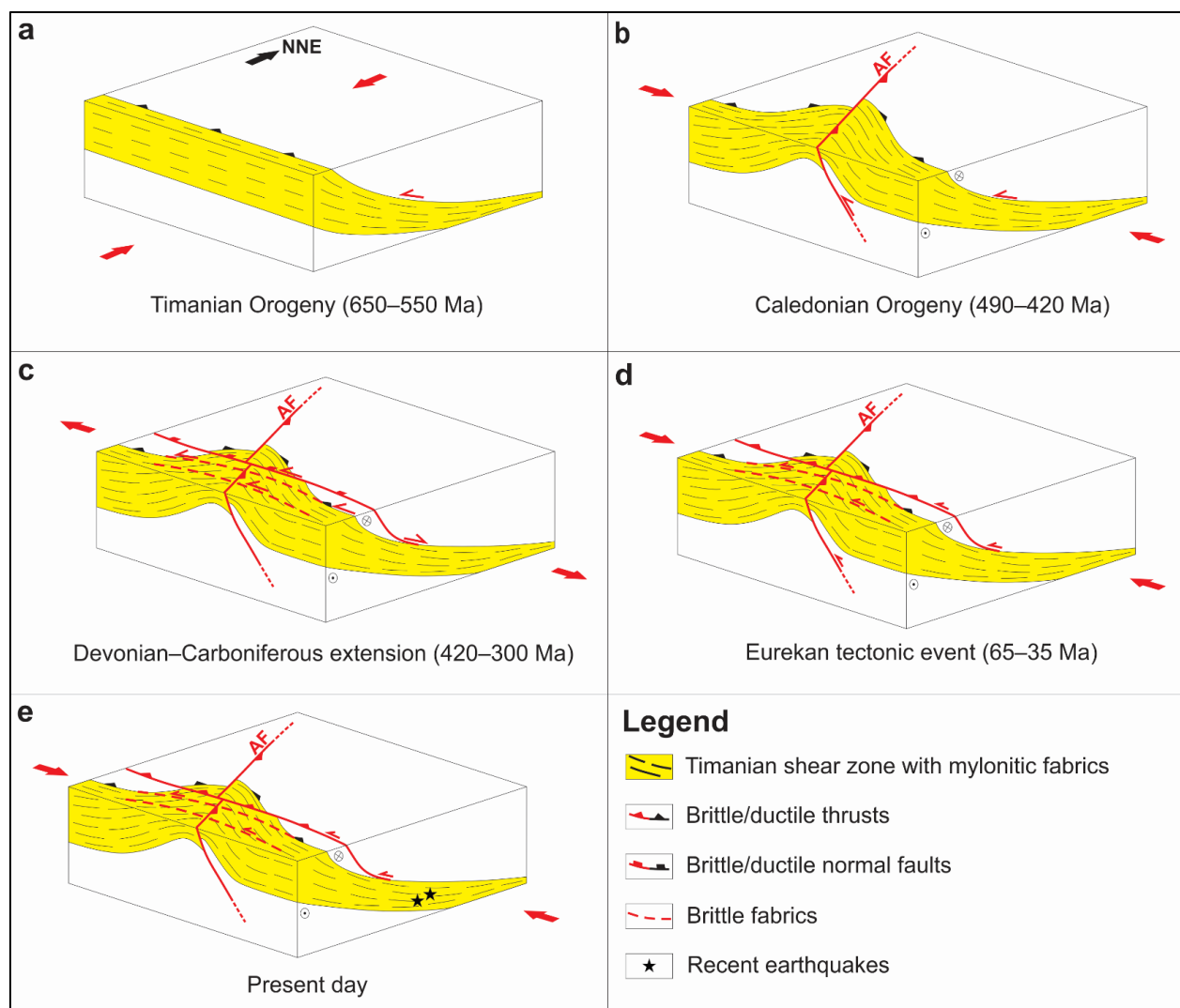


Figure 7: Tectonic evolution of Timanian thrust systems in eastern Spitsbergen, Storfjorden and the northwestern Norwegian Barents Sea including (a) top-SSW thrusting during the Timanian Orogeny, (b) reactivation as oblique-slip sinistral-reverse thrusts and offset by top-west brittle thrust overprints (e.g., Agardhbukta Fault – AF) under E–W contraction during the Caledonian Orogeny, (c) reactivation as low-angle, brittle–ductile, normal–sinistral extensional detachments and overprinting by high-angle normal–sinistral brittle faults during Devonian–Carboniferous, late–post-Caledonian extensional collapse and rifting, (d) reactivation as brittle–ductile sinistral–reverse thrusts, overprinting by high-angle sinistral–reverse brittle thrusts, and mild offset by reactivated top-west thrusts (e.g., Agardhbukta Fault – AF) during E–W Eurekan contraction, and (e) renewed, recent–ongoing, sinistral–reverse reactivation and overprinting possibly due to ongoing magma extrusion and transform faulting (ridge-push?) in the Fram Strait.

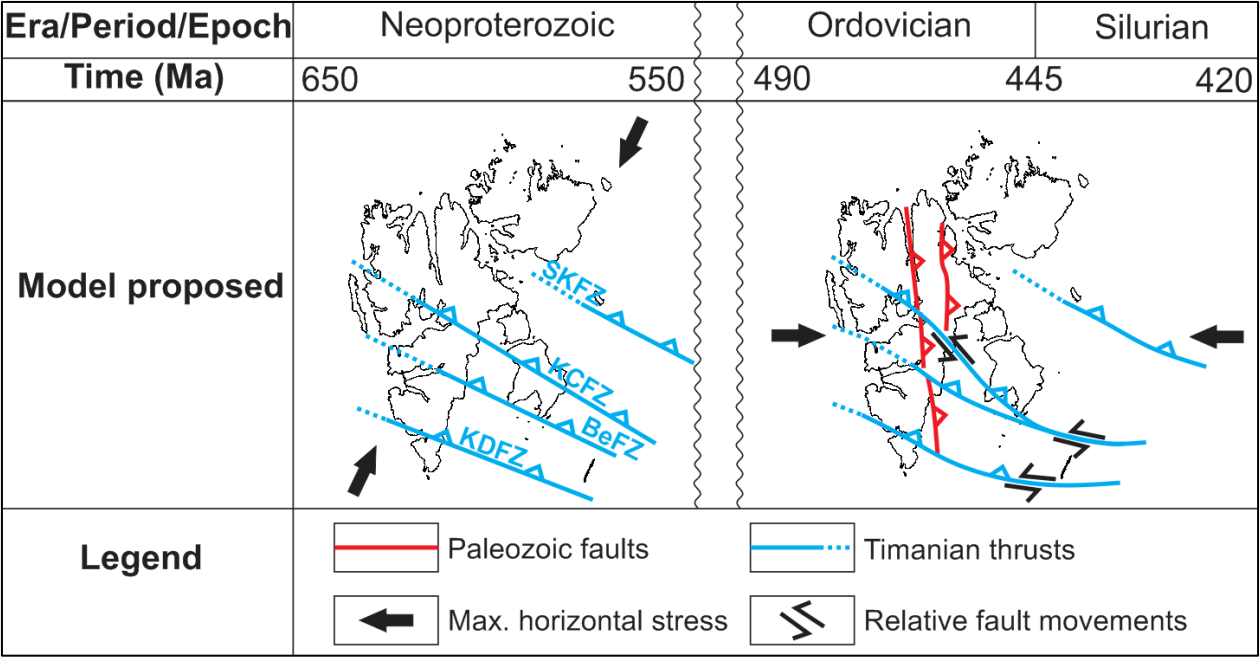


Figure 8: Paleogeographic reconstruction of the Svalbard Archipelago in the latest Neoproterozoic during the Timanian Orogeny and in the early–mid Paleozoic during the Caledonian Orogeny according to the present study.